Development and validation of a novel device for the culture of spheroids

Mina Lotfi Kelahrodi

Anatomy and Cell biology department, Faculty of medicine, McGill University, Montreal

August 2020

A thesis submitted to McGill University in partial fulfillment of the requirement of the degree of Master of science (M.Sc.) in anatomy cell biology

Table of contents

Table of contents
Table of figures5
Table of tables6
Abstracts
Abstract (English)
Résumé (Français) 8
Acknowledgements9
Contribution of authors
Section 1. Review of relevant literature
1. Review of Relevant Literature
1.1. Cell signaling
1.1.1. Cell-cell communication
1.1.1.1. Notch pathway
1.1.1.2. Gap junction
1.1.2. Cell-ECM communication
1.1.2.1. ECM composition
1.1.2.2. Integrins: Mediators ECM-cell signaling
1.2. Cell culture approaches
1.2.1. 2D cell culture
1.2.2. 3D cell culture
1.2.2.1. Scaffold-based technologies
1.2.2.2. Non-scaffold-based 3D cell culture
1.3. Current non-scaffold-based 3D culture systems

	1.3.	1. Hanging drop (HD)	. 29
	1.3.2	2. Ultra-low adhesion plates	. 29
	1.3.3	3. Magnetic levitation	. 30
:	1.4.	Microfluidic devices	. 30
	1.5.	Differences between 2D and 3D cultures	. 31
Section	ı 2. Ra	tionale and objectives	. 33
2.	Rati	onale and objectives	. 34
:	2.1.	Rationale	. 34
:	2.2.	General objective	. 36
:	2.3.	Specific objectives	. 36
:	2.4.	Hypothesis	. 36
Section	1 3. Ma	aterials and methods	. 37
3.	Mat	erial and methods	. 38
;	3.1.	Cell culture	. 38
:	3.2	Fabrication of the devices	. 38
	3.1.	1. Computer-assisted design (CAD)	. 39
:	3.2.2	3D printing	. 41
:	3.6	Spheroid growth measurement	. 46
:	3.7	Processing of spheroid for whole-mount immunofluorescence microscope	. 46
	3.7.	1 Fixation	. 46
	3.7.2	2 OCT mounting	. 46
	3.7.3	3 Hematoxylin and Eosin (HE) staining	. 47
	3.7.4	4 Live-microscopy Staining	. 47
,	3	Canillary numn	48

	3.9	Imaging	49
Sectio	n 4. Re	search findings	50
4	Res	earch findings	51
	4.1	3DForCell version 1.0	51
	4.2	3DForCell version 2.0	52
	4.3	3DForCell version 3.0	53
	4	.3.1 Effect of ethanol and long-term ethanol incubation on devices	54
	4	.3.2 Test 3D ForCell version 3 cell seeding, No spheroid?	55
	4.3.	3 3DForCell version 4.0	58
	4	.3.3.1 Cell seeding from top of culture chamber in 3D ForCell version 4.0	60
	4	.3.3.2 Can we improve 3D ForCell fabrication?	61
	4.3.	4 3DForCell version 5.0	63
	4.4	Capillary pump	65
Sectio	n 5. Di	scussion	67
5	Disc	cussion	68
	5.1	Design	68
	5.2	Printing and fabrication	69
	5.3	Growing spheroid	70
	5.4	Capillary pump	71
Sectio	n 6. Co	nclusions and future perspectives	72
6	Con	clusions and future perspectives	73
	6.1	Conclusion	73
	6.2	Future perspectives	75
Refere	ences		77

Table of figures

Figure 1. Schematic view and picture of 2D and 3D cell cultures	19
Figure 2. The 3D ForCell fabrication models	35
Figure 3. Main steps in the preparation of 3D ForCell devices.	39
Figure 4.Different versions of 3D ForCell devices	40
Figure 5. All 3D printer models.	42
Figure 6. Anycubic photon LCD-based SLA 3D printer	43
Figure 7. Cell seeding from the media chamber and the top of culture chamber	45
Figure 8. Cassette strip with filter paper	48
Figure 9. Steps of changing media with a paper-based capillary pump	49
Figure 10. The 3DForCell version 1	51
Figure 11. 3D ForCell device version 2	52
Figure 12. 3D ForCell version 3.	53
Figure 13. Cracks presented in the 3D ForCell device.	54
Figure 14. Test sterlization protocol.	55
Figure 15. Cell seeding attempt in version 3	55
Figure 16. Compare 3D ForCell device and ULA plates	56
Figure 17. H&E staining images from MCF7 spheroid	57
Figure 18. Fluorescence labeling.	58
Figure 19. 3D ForCell device version 4	59
Figure 20. Test the 3D ForCell device version 4 without cells	60
Figure 21. Spheroids growing in 3D ForCell v4.0.	61
Figure 22. Compared version 4 and 5 of the 3D ForCell	63
Figure 23. Version 5 model a to c	64
Figure 24. Black 3D ForCell device	64
Figure 25. DIC and confocal images from spheroid into two different conditions	65
Figure 26. Perfusion rate of versions 3 and 5 of the 3D ForCell device	66

Table of tables

Table 1. Properties of in vitro 3D cell culture models	28
Table 2. Size variation in composition of the 3D ForCell device versions	40
Table 3. Examples of the post-processing conditions tested.	62

Abstracts

Abstract (English)

Introduction: We seek to develop and validate a 3D cell culture system that provides a low-cost and user-friendly method to culture spheroids. This new 3D-printed device, 3DForCell, contains a media chamber and a microfluidic channel to facilitate media exchange with a culture chamber, an air vent, and a paper-based capillary pump can be used to change media. The device uses a media-oil interface to suspend cells and promote aggregation without the usual problems of hanging-drop systems using a media-air interface. This device is an improvement in existing systems such as hanging drop, ultra-low adhesion plates, and magnetic levitation, which comes with difficulties in changing media and manipulating spheroids for processing or imaging.

Hypothesis: This novel device is a better alternative than pre-existing techniques for the generation of the spheroid.

Methods: The devices were designed via SolidWorks, and printed with a stereolithography, LCD-based 3D-printer from Anycubic (Photon). In the perfusion test, different filter papers with different thicknesses were used to choose the slower one to absorb media.

Results: We developed this device through an iterative process that covered 5 individual versions. We got moderate success with the last two designs as we were able to grow spheroids. The final designs had a glass coverslip, a bigger media chamber, UV glue, bigger culture chamber, and a thicker media chamber. In the perfusion test, the filter papers number 1 and 2 have a slower flow rate to change media.

Conclusions: This microfluidic device has many advantages to use for the spheroid generation due to be user-friendly and cost-effective. It could also solve some problems in the current non-scaffold 3D cell culture systems such as ULA-plates, hanging drop, and magnetic levitation.

Résumé (Français)

Introduction: Nous présentons ici les travaux entourant le développement et la validation d'un nouveau système de culture cellulaire tridimensionnel économique et facile d'utilisation pour la cultivation de sphéroïdes. Ce nouveau dispositif, 3DForCell, contient un puit contenant le milieu de culture relié à une chambre de culture par un micro-canal facilitant le changement de milieu de culture par le biais d'une pompe a échange capillaire en papier. Il comprend aussi une chambre contenant de l'huile biocompatible, qui par le biais de la création d'un interface huile-liquide, permets de créer une surface concave promouvant l'agrégation cellulaire et la formation de structure sphéroïdales. Ce nouveau système, en plus de faciliter l'échantillonnage et le changement de milieu de culture, pourrait avoir l'avantage d'être plus stable que les systèmes en goutte-suspendue traditionnels utilisant un interface air-liquide.

Hypothèse: Ce nouveau dispositif constitue une nette amélioration par rapport aux techniques existantes pour la génération et la culture de sphéroïdes.

Méthodologie: La conception de toutes les versions de ces dispositifs a été faite via SolidWorks. La microfabrication a été faite par impression 3D par stéréolithographie via une imprimante à résine utilisant un écran LCD (Anycubic; Photon). Les tests de perfusion ont été effectués avec des papiers filtres traditionnels d'épaisseurs diverses.

Résultats: Le développement des dispositifs 3DForCell fut itératif et inclus 5 versions. Des succès modérés ont été obtenus avec les deux dernières versions; nous avons réussi à obtenir plusieurs sphéroïdes. Le design final était constitué d'une lamelle de microscope collé par une résine UV, ainsi que d'un puit de milieu et d'une chambre de culture agrandit. Le débit le plus lent fut obtenu avec les grades de papier filtre 1 et 2.

Conclusions: Ce dispositif microfluidique possède plusieurs avantages pour la génération et la culture de sphéroïdes. Ceci pourrait également résoudre certains problèmes reliés aux technologies existantes comme les plaques à ultra-basse adhésion, à goutte suspendues, ou à lévitation magnétique.

Acknowledgements

This master thesis could not have been done without support of McGill faculty of medicine scholarship. I would like to thank Dr. Lorraine Chalifour and Dr. Aimee Ryan, Graduate associate deans of McGill university, as justice seeker scientists who supported my career aims. No appropriate words can express my respect and thank my supervisor Dr. Craig Mandato, chairman of the department of Anatomy & Cell biology, whose expertise and support allowed me throughout the project from the first until the last steps. My sincere acknowledgement goes to Dr. Eric Boucher, research associate & lab manager of Dr. Mandato lab. He is such as morale, fair, and helpful guy who trained me technical experiments and supported me in troubleshooting and thesis preparation.

I would like to extend my thank to my committee members for their guidance. Dr. Susanne Bechstedt as the best mentor I could have. Her encouragement provided me more motivation to continue my way. Dr. Chantal Autexier, as the blessing of the Anatomy & Cell biology department, which supports all graduate students, especially me, to pursue our goals. Dr. Allen Ehrlicher, provide me an opportunity to have collaborate with his lab members about my project.

I am most grateful to Dr. Hojatollah Vali for his generous support and Dr. Jamal Daoud as an innovative scientist for their interesting project, 3D ForCell device. Special thanks to peers in the lab, including graduate students David Zhou, Quentin Basiren, and undergraduate student Jason Jang, to make helpful discussions and nice academic time.

I am appreciated to my former supervisors, Dr. Morteza Mahmoudi, associate professor at Michigan university, Dr. Nasser Aghdami, head of cell therapy in Royan institute, Dr. Behnam Sadeghi, assistant professor in Karolinska institute, Dr. Nader Haghighipour, professor at NASA, for their warm support and positive words during past years. I would like to acknowledge my friends who helped me in hard times, cheered me on, and pushed me to continue my way: Nazanin Hoshyarjah, Nima Akbarzadeh, Tanzila Wasi, Jingyu Sun, and Swathi Adinarayanan.

Finally, I deeply thank my family, especially my parents, for their love, trust, and endless patience.

Their encouragement helped me raised up again when I felt frustrating cold despite being in long distance.

Contribution of authors

<u>Introduction</u>

Mina Lotfi prepared and wrote the manuscript.

Materials and methods

Mina Lotfi prepared and wrote the manuscript and adapted protocols existing in the Mandato lab or provided by J.Daoud.

Results

Mina Lotfi prepared and wrote the manuscript, performed the experiments, and analyzed the data. Mina Lotfi contributed to the overall experimental design, with the help of E. Boucher, J. Daoud, and Prof. Craig Mandato.

<u>Discussion and Future perspective</u>

Mina Lotfi prepared and wrote the manuscript.

Section 1. Review of relevant literature

1. Review of Relevant Literature

1.1. Cell signaling

Cell signaling refers to the ability of cells to communicate with neighboring cells and the surrounding extracellular matrix (ECM) in order to coordinate cell actions and to respond to external cues. The interaction of ECM and cells is an important feature to support some cellular behaviors like proliferation, cell migration, differentiation, apoptosis, and gene expression [1]. The cell signaling errors may lead to some diseases such as cancer or immune dysfunction [2].

In multicellular organisms, there are two main types of cell signals: mechanical and chemical. Mechanical signals refer to the ability of cells to sense the physical forces of the surrounding environment and react to the applied force [3]. Chemical signals are classified into four groups based on the distance that signals are transmitted to reach the targeted cells.

Autocrine signals release from the signaling cells and affect themselves via receptors like immune responses [4].

Paracrine signals are signals that act on the neighboring cells. The response of this type of signal is speedy and the signal can be removed from the targeted cells in a short time. The neurotransmitter in nerve cells is an example [5].

Endocrine signals are a type of signals which have a longer distance to reach to targeted cells and create a more prolonged effect. All the hormones in the body are endocrine signaling molecules that travel through the bloodstream and affect the long-distance cells [4].

Juxtracrine signals are direct contact between cells to an adjacent cell. These interactions can be between a protein of one cell to a receptor of neighboring cell or between cell's receptor to ECM ligand of an adjacent cell, and between the cytoplasm of two cells [5].

1.1.1. Cell-cell communication

1.1.1.1. Notch pathway

One of the main pathways for cell-cell communication goes through notch signaling. Notch is a type of receptor on the surface of the cell and Delta, Jagged, and Serrate are ligands expressed on the surface of adjacent cells. These three proteins Delta, Jagged, and Serrate present in most multicellular organisms. By expressing these proteins in the cell membrane of cells, the external components of them are represented as ligands into outside and can activate the notch signaling in adjacent cells. Binding between notch signaling receptors and external components of ligands in induced cells can activate protease to cut the notch signaling pathway. The cleaved proteins connect to the nucleus to capture other DNA-binding proteins and activate their gene expression [5].

Notch signals are vital to cell networking during the embryonic and adult lifetime, especially in the nervous system. For instance, during the embryonic step of the vertebrate eye development, the notch pathway coordinates cell fate to choose which one becomes optic or glial neurons [6].

1.1.1.2. *Gap junction*

Another cell-cell communication pathway transmits signals from the cell membrane of one cell directly into the adjacent cell membrane via structures named gap junctions. In this mechanism, inorganic ions and small metabolites (molecular weight <1500) transmit from cell to neighboring cell through a channel made from connexin proteins.

Gap-junctions composed of connexin proteins and assemble hexameric structures of connexin proteins make connexon. When the connexon of one cell is fused to a partner connexon in parallel from adjacent plasma cell membranes, they form an intracellular channel. Few to many of these connexons can assemble to each other and make a gap junction. In other words, assembly, disassembly, and remodel of intracellular channels made from connexons give a dynamic structure to gap junction. The dynamic gap junctions provide direct electrical and chemical communication between cells [7]. Electrical transmission between neuron cells was the reason to identify gap junction in nerve cells. In this case, gap junction allowed to transmit

electrical signals from cell to cell with higher speed [8]. However, it does not mean the gap junction just works in electrically excitable tissues; for instance, the liver coordinates transmitted signals from neuron terminals in their cells using gap junction. An example of chemical communication between cells by gap junction can be mentioned in damaged cells. When the plasma membrane is damaged, the exogenous cations such as Ca2+ and Na+ move in and can destroy the cell. If the gap junctions between adjacent cells do not close rapidly, those cells will suffer from extra cations distributions into them. However, the gap junction channel will close quickly after cell-damaging and the ions concentration will remain balance in adjacent cells [7].

1.1.2. Cell-ECM communication

Advances in cell biology revealed that ECM is closely connected to cells residence in both structure and behavior. The cells surrounded the matrix, secrete the macromolecular components of the ECM. They also play roles in the organization and behavior of the matrix after secretion. Therefore, the cell-ECM connection makes important interactions in connective tissue. Cell-ECM communication is important not only in vivo but also important in both 2D and 3D cell cultures (Section 1.5).

1.1.2.1. <u>ECM composition</u>

Approximately 90% of components of the ECM consist of proteoglycans and are involved in cellular functions such as cell-cell, cell-ECM interconnections. Glycoprotein found in ECM can be divided into two groups: collagens and non-collagens proteins (reviewed in [9]).

Collagens are the most abundant components of the ECM and the biggest contributors concerning the structural integrity and physical properties of the ECM. Collagen also contributes to other cell prosses, such as cell adhesion and migration support, strengthen, and tissue development [10]. It formed from triple-helical conformations, which are rich in proline and glycine acid amines. In addition, collagen has a superfamily that 28 types of them have

been identified until now [11]. The most common structure of collagen is a fibrillar formation, which can be found in I, II, and III types. The structural composition of skin, tendon, and bone is formed from collagen type I and also the cartilage structure mainly formed from collagen type II. In addition, the most collagenous structure in all tissues of the body constitutes of collagen type VI [12]. Not only collagens form major components of the ECM compositions, but also they play roles in storage and carry growth factors and cytokines in tissues [13].

Another important macromolecular of the ECM in connective tissues are glycosaminoglycans (GAGs) [7]. GAGs are polysaccharides contained repeating disaccharides with an amino sugar (N-acetylglucosamine or N-acetyl galactosamine) and a uranic acid (glucuronic or iduronic) components. GAGs have four main groups, which are categorized by type and location of sugars and sulfate. These groups include chondroitin sulfate and dermatan sulfate, heparin and heparan sulfate, hyaluronan, and keratan sulfate [14].

GAGs have negative charges due to the existence of sulfate or carboxyl groups on the disaccharide components. This negative charge causes cells to absorb cation ions, especially Na+, in GAGs, which leads to a significant amount of water in porous parts of the matrix. This hydrodynamic the matrix to tolerate more atmosphere pressures [7].

Proteoglycans (PGs) are types of proteins attached to all GAGs, except hyaluronan, which produced with the expression of fewer than 50 genes (reviewed in [15]). The main difference between proteoglycan and glycoprotein is the amount of carbohydrates, which is around 95% in PGs and near 1-60% in glycoproteins [7]. In addition, PGs are attached to GAGs chains on one side that plays a role in PGs functionality. The main role of PGs is in chemical signaling of the cells, such as growth factors, cytokines, chemokines, inflammatory response, and cell-cell communication (Reviewed in [15, 16]).

Some well-known non-collagenous glycoproteins of the ECM are laminin and fibronectin. The basal lamina is a type of ECM that always lies at the surface of epithelial cells and connective tissue, which mainly composed of laminin [17]. Laminin is involved in ECM assembly, cell adhesion and migration, and cell morphology [18]. Fibronectin is a large glycoprotein secreted by cells which has several binding sites to link with other molecules such as fibronectin,

collagen, and other proteoglycans. Therefore, several biding sites in fibronectin provide it important role in cell adhesion and migration [19], especially in cardiovascular development and cancer metastasis [20, 21].

1.1.2.2. <u>Integrins: Mediators ECM-cell signaling</u>

ECM is linked to the cytoskeleton of cells by one of the major families of receptors named integrins. In invertebrates, 24 different integrins have been identified. Integrins are heterodimeric receptors consisting of pairings of 18 α with 8 β transmembrane glycoprotein subunits [22]. The integrin structure shows three main fragments: a large extracellular ligand-binding fragment, a transmembrane glycoprotein fragment, and a cytoplasmic section to transduce cell signaling [23]. The Integrins subunit's distribution is different in tissues of vertebrate cells. For instance, β 1 subunits are distributed everywhere of all mammalian cells. However, β 2 subunits are found in white blood cells [7]. The integrity of cell-ECM has been preserved by Integrin receptors due to control outside-in and inside-out signaling pathways [24].

Integrin mediates the interaction between the exterior and interior of the cell. The extracellular domain of integrin is connected to the extracellular matrix and the cytoplasmic domain is attached to the actin filament of the cytoskeleton. Therefore, integrins control signaling in and out in the cells, which have a role in common cellular functions such as adhesion, migration, proliferation [7].

Focal adhesions (FAs) structure, which contains integrins as components, mediate outside-in signaling. FAs are physically linked between the extracellular matrix out of the cells and the actin cytoskeleton in the inner of cells. FAs have the ability to transfer mechanotransductive ECM signals through integrin activation into the cells. There are over 150 proteins in FAs, such as focal adhesion kinase (FAK) and Src proteins [25].

The outside-in signaling pathway starts when the cytoplasmic domain of integrin is activated from the outside domain with autophosphorylation of FAK, which binds with Src protein. The inside domain of integrins is bounded to intracellular proteins such as talin, α -actinin, and filamin, which directly connect to the actin of cytoskeleton [26]. From these direct linker

proteins, talin has a critical role in downstream activation of integrins with binding to the integrin B cytoplasmic domain (Reviewed in [27]). This critical element has sites for other proteins named linker proteins indirectly to physically bound integrin to the cytoskeleton [28]. The indirect linker proteins in FAs include vinculin, nexilin, ezrin-radixin-myosin proteins [29]. Recently, research showed the Rho family of GTPase could help to localization of Src protein to actin intracellular area [30], stimulate FAs to develop and move forward [31].

1.2. Cell culture approaches

1.2.1. <u>2D cell culture</u>

In 1907, for the first time, Harrison carried out 2D cell culture on cells derived from neuroblasts [32]. This method provided much information for scientists about how cells grow, proliferate, and differentiate in *in vitro* environment. In adherent 2D cell cultures, cells are typically built on a rigid plastic or glass surface optimized for attachment and proliferation of cells in flasks and petri-dishes [33]. Oxygen and a metabolite source, such as nutrient-rich media are required grow cells in 2D culture. To simulate body temperature (37°C), incubators are used to maintain a warm environment. Cells can thus proliferate in plastic flasks until they reach confluency. If cells confluency goes over 80-90%, it can influence their health and changes the expression of certain genes [34]. Thus, when cells reach 70-80% confluent, they have to re-seeded by the use of trypsin and EDTA, which releases them from the plastic substrate of the flask. By counting the cells, the proper concentration of cells re-seeded into new commercial polystyrene plastic flask to continue cell line passages. This system is simple, fast, and cost-effective. However, the biggest problem is its limited range of cell-cell contacts and cell-ECM interactions. Therefore, 2D cell cultures do not perfectly imitate the 3D in vivo model and tumor architecture [35].

1.2.2. 3D cell culture

While the 2D cell culture technique has provided much information, it is not entirely successful in mimicking the *in vivo* physiological microenvironment [36]. Some of the drugs have failed In clinical trials phases II or III because of 2D cell culture data could not provide an acceptable prediction of drug efficacy and safety [37, 38]. One of the biggest problems in 2D cell culture is the lack of cell-cell and cell-extracellular matrix (ECM) interactions[39]. Therefore, the tumor biologists have launched their research to develop the new *in vitro* culturing model to replace traditional 2D cell culture. Dr. Mina Bissel (an Iranian-American breast cancer biologist) from the Lawrence Berkeley National Laboratory was one of the first to established 3D cell culture techniques resembling a natural *in vivo* environment [36, 40].

Over the past decade, emphasizing the importance of tumor studies has dramatically increased 3D cell culture model advancement. The wide range of research has proven that 3D cell culture technology can imitate the physiological conditions such as cell-cell and cell-ECM interactions, morphology, polarity, proliferation, differentiation, migration, apoptosis, and cell signaling [41]. 3D cell culture is categorized into two groups: scaffold- and non-scaffold-based systems (Figure 1. A).

The scaffold-based systems using types of physical support can closely resemble cell-ECM interconnections found *in vivo*. In this system, cells are embedded in a scaffold that is already prepared (Figure 1. A). The non-scaffold- based systems recapitulate the tissue and cancer environment, which seems to be more appropriate to mimic physiological conditions. In this system, cells secrete their own ECM and make self-assembly without the need to use external support (Figure 1. B) Both of these systems provide cell-cell and cell-ECM interconnection, which is not present in the 2D cell culture system [42, 43].

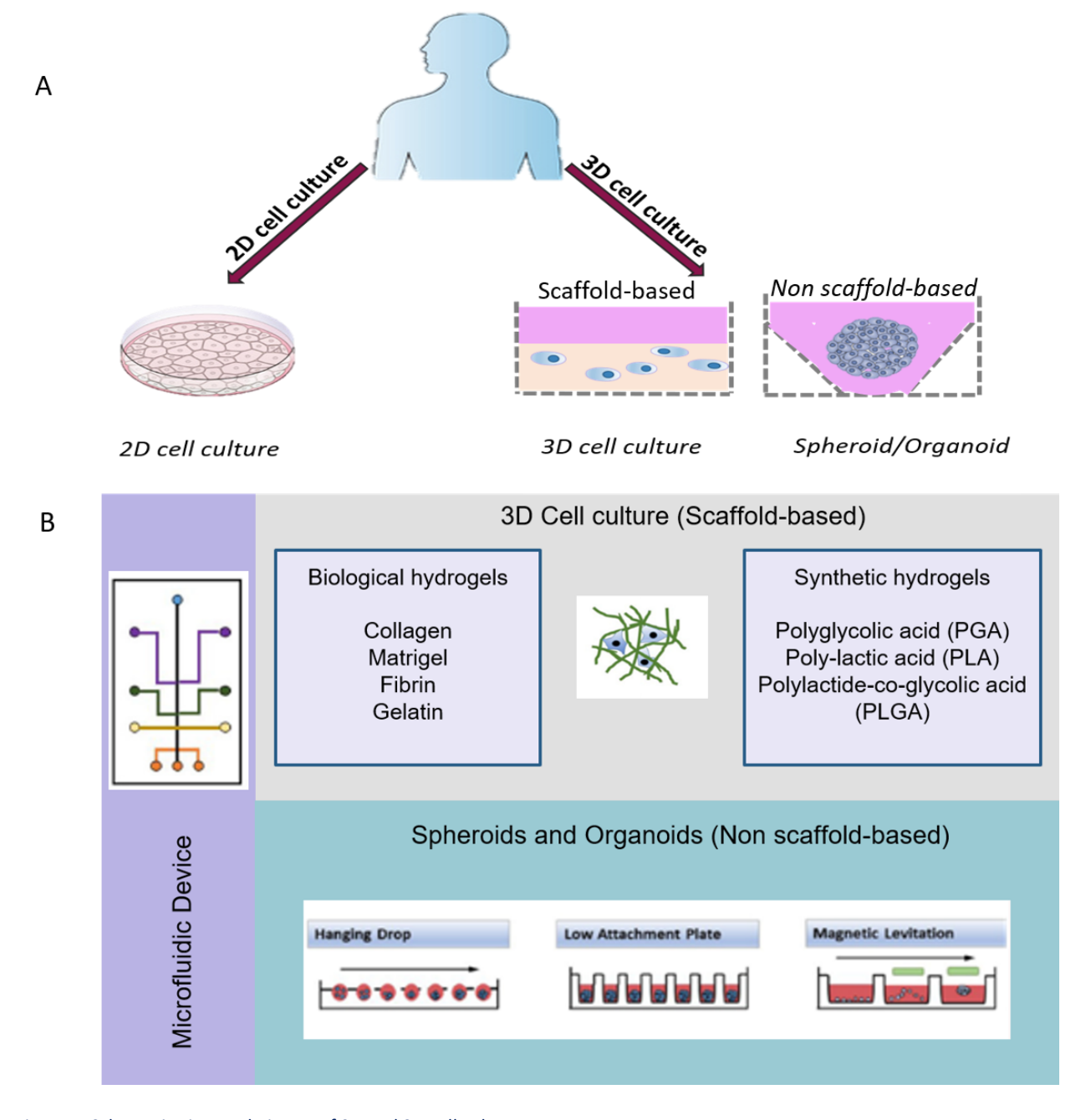


Figure 1. Schematic view and picture of 2D and 3D cell cultures.

This figure modified from [42], with permission form the author and the publisher (Experimental Pharmacology and Drug Discovery).

A) In 2D cell culture, cells are plated in a rigid plastic surface. However, 3D cell culture, which derived in scaffold-based and scaffold free-based systems, cells are cultivated in environment more similar to in vivo. B) Scaffold-based 3D cell cultures categorized into two groups biological and synthetic hydrogels. Non-scaffold-based system creates spheroid and organoid in 3 current models such as hanging drop, low attachment plate, and magnetic levitation.

1.2.2.1. Scaffold-based technologies

1.2.2.1.1. <u>General characteristics</u>

In scaffold-based 3D culture, cells are embedded in natural or synthetic scaffolds [44] (Figure 1B). The scaffold-based system is considered to be necessary to maintain typical cellular structures and processes, such as growth, aggregation, proliferation, differentiation, and migration dependent on ECM interactions [42]. These materials should mimic biocompatibility, biodegradability, stiffness, and porosity features of the ECM of a given tissue[45]. However, these features of the biomedicals used in scaffold-based 3D-culture affect cells in various ways [46].

Stiffness relates to the resistance response of biomaterials whenever physical force was applied [47]. Young's modulus (E) is a measurement assessing the stiffness of materials [48]. The elastic properties of biological tissues are in a wide range: from very soft brain and lung tissues (E=1-10 KPa) to tough and rigid bone tissues (E= 2-4 GPa) [48]. The nature of ECM has an influence on the mechanical properties of tissues. Research has shown that tissue or ECM stiffness also a role in stem cell differentiation [49]. For example, cultivation of mesenchymal stem cell on top of soft polyacrylamide gels (E= 0.1–1 kPa) leads to their differentiation into neuronal cell-type, culture on relatively stiff gels (E= 8–17 kPa) leads to their differentiation into muscle cells, and culture with even more rigid gels (E= 25–40 kPa) leads to their differentiation into a bone lineage [50].

The porosity is one of the scaffold features that can influence cell fate as it provides an environment for mechanotransduction signals and the perfusion of nutrients and oxygen. The pore size also has an essential role in cell adhesion and migration. High porosity can provide more surface area for cell-matrix interactions, space for ECM regeneration, and allows for efficient cell seeding [51]. In addition, cell adhesion and ease of cell growth in the scaffold can be dependent on pore properties. For instance, *in vitro* model by seeding primary rat osteoblast into styrene foams, the smaller pore size (40 μ m) kept more cells; however, the larger pore size (100 μ m) revealed faster cell migration speed. The small pore size of polyethylene terephthalate fibers with thinner diameters (9 and 12 μ m) showed higher proliferation in rat mesenchymal stem cells (reviewed in [52]).

Compatibility means choosing biomaterials that do not have unwanted side effects in the cell regeneration process and do not have cytotoxic effects [48]. The scaffold also should be made from biodegradable material, which ensures provides appropriate remodeling of the desired tissue. In fact, the degradation of scaffolds, both in vitro and in vivo conditions, leads to release by-products [53].

Scaffold-based 3D cell culture derived into two main groups: biological and synthetic origins (Figure 1. B). The biological scaffolds have more biodegradability, lower immunogenicity, and providing positive support for cell functionality. However, synthetic scaffolds have lower biodegradability, but possess higher versatility, reproducibility, and are easier to process [54].

1.2.2.1.2. <u>Biological hydrogels</u>

Hydrogels can be made or derived from natural biomaterials, including collagen, alginate, hyaluronic acid, cellulose, fibrin, or gelatin. They maintain natural cell features such as adhesiveness, viability, and controlling cell proliferation and differentiation. Besides, they have high biocompatibility and biodegradability [55].

Collagens

The most common biological hydrogel is used as a scaffold for embedding in 3D cell culture is collagen. Collagens are a family of proteins that have a role in ECM integrity and connective tissue [13]. The main structure of collagen is formed from the polypeptide chain with a repeating the triple unit of amino acids, which mostly contain glycine, proline, and hydroxyl proline [56]. The mechanical strength of tissues depends on the specific type of collagen (e.g., type I, II, III, V, and XI) [57], which be extracted from different tissues including bone, cartilage, skin, tendon [48].

Collagen has fibrillar conformation, which outside of isoelectric PH becomes to gel. The gel formation is between liquid and solid form. By crosslinking of collagen gel can obtain hydrogel form. This crosslinking can be formed by making a bond between fibrils of the gel [58].

Collagen can facilitate cell attachment, which causes to the regulation of signaling pathways to control cell proliferation, differentiation, and migration [59]. The low toxicity, good permeability, and high biocompatibility and biodegradability properties made collagen as a promising. For instance, using collagen as a hydrogel to the 3D cell culture of breast cancer cells, those tumor model cells have demonstrated more similarity to the architecture and cellular heterogeneity of typical breast cancer cells *in vivo* [60].

Although, the collagen hydrogels have revealed a lack of mechanical strength and architecture stability upon hydration. Therefore, the late weakness leads to limitations to choose them as a scaffold for particular tissues [61].

<u> Matrigel</u>

Matrigel, similarly to collagen, can provide ease of cell adhesion feature and controlling cell survival, growth, and differentiation by activating the notch cell signaling pathway [42]. Matrigel is a gelatinous mixture of proteins consisting laminin, collagen IV, entactin that can also include some cytokines and growth factors such as EFG (epidermal growth factor), bFGF (basic fibroblast growth factor), NGF (nerve growth factor), IGF-1 (Insulin-like growth factor1) and TGF- β (transforming growth factor- β) [62].

The component proteins in Matrigel provide it as a qualified hydrogel for cell culture. For instance, bone marrow stem cells (BMSCs) can be cultured on Matrigel for more than five months in comparison to the BPS control group [63]. Another research on Tonsil derived mesenchymal stem cells (TMSCs) showed that survival rate of those cells on this type of hydrogel enhanced 40-80% [64]. Drug testing has also been done in 3D Matrigel cell culture, more specifically on cultured non-small lung and colorectal cancer cells. Matrigel is also suitable for cancer stem cells (CSCs) cultivation. For instance, breast cancer stem cells cultured on Matrigel could express a new transmembrane glycoprotein named nicastrin [65]. Other research demonstrated that intestinal cancer cells derived from mice are able to be maintained for up to 350 days in a Matrigel matrix [66]. 3D Matrigel cell culture of non-small lung cancer

has revealed important matrix invasion and mechanotransduction signaling, which led to metastasis-related morphologic and gene expression responses [67].

However, there are some drawbacks of using Matrigel scaffold, including it tends to be expensive, and that their complex composition can vary widely [68].

<u>Fibrin</u>

Fibrin is a natural polymer in wound healing which is derived from fibrinogen. Fibrin has biocompatibility, degradability, and dissolvability abilities, which make it a well-known material to use as a hydrogel in tissue engineering.

In last decades, a variety of 3D cell culture applications have been applied to fibrin biomaterial as a hydrogel such as bone [69], cartilage [70], skin [71], liver [72], cardiovascular [73], adipose tissue [74], [75]. In addition, fibrin has been utilized as a bioink base for printing neural cells in drug screening of glioblastoma, Schwann cells for nerve tissue engineering, human dental pulp stem cells for tooth 3D cell culture, and MSCs for bone tissue engineering [48].

However, the fibrin scaffolds have shown some limitations such as rapid degradation even before tissue formation, low stiffness, and high shrinkage rate during flat sheet formation [76].

<u>Gelatin</u>

Gelatin is a promising natural biomaterial as a scaffold derived from collagen due to chemical similarity to natural ECM. It has high compatibility, degradability, adhesiveness, low toxicity, cost-effectiveness with various melting points, and viscosity regarding the origin of gelatin derived from which animals [77].

Gelatin has poor mechanical properties, which means the shape of gelatin is thermoreversible. Based on the temperature, the form transit between solid and liquid form. Gelatin has liquid shape when it is cooled and has solid formation when heated (Reviewed in [77]). This feature makes a hard situation to print it. Therefore, to optimize printability, gelatin has been combined with other biological hydrogels [78] such as alginate, cellulose, hyaluronic acid, or synthetic polymers, including PCL [79], PEG [80], PLLA [81].

1.2.2.1.3. Synthetic hydrogels

The ideal synthetic hydrogel should mimic natural ECM properties, as well as having bioinert, biodegradable, and biocompatible features [82]. Meanwhile, they have to contain a desired stiffness and porosity for specific applications [83]. The most significant advantage of a synthetic hydrogel is that it can be manufactured under controlled conditions. It means synthetic hydrogels' chemical and physical properties can be predictable and repeatable, including elasticity and degradability features [82]. Also, some hormones, growth factors, and biological molecules can be encapsulated in synthetic hydrogels to increase cell proliferation and differentiation [84].

The more common synthetic materials are poly-lactic acid (PLA), polyglycolic acid (PGA), and polylactide-co-glycolic acid (PLGA). All of these polymers have revealed good biodegradability, biocompatibility, and versatility in pharmaceutics tests (Reviewed in [85], [86]). Based on the specific applications, they have to design suitable shapes and pore sizes [55].

The degradation rate of PGA is higher than PLA due to its more hydrophilic properties [87]. Variation in molecular weights and copolymers can be used to adjust the physical and chemical properties and degradation rate of PLA and PGA. However, these polymers undergo a bulk erosion process such that they can cause scaffolds to fail prematurely. In addition, the sudden release of these acidic degradation products can create a robust inflammatory response [88].

PLA and PLGA have been used as hydrogels in many inorganic materials, and they have high degradability property. However, these polymers have been shown to exhibit a toxic influence on cell culture systems in 3D cell culture for high concentrations [89].

1.2.2.2. Non-scaffold-based 3D cell culture

In non-scaffold-based systems, cells assemble into organized 3D tissue structures [90] on their own. Scaffold-free systems closely recapitulate the in vivo microenvironment due to ECM secretion by the cells. Specialized techniques such as hanging drop, ultra-low attachment plates, magnetic levitation, and the microfluidic device can be used to force cells to be aggregate and create 3D cellular structures called organoids and spheroids [91] (Figure 1. B).

1.2.2.2.1. Organoids and spheroids

Organoids are self-organized 3D cultures derived from embryonic stem cells (ESCs), induced pluripotent stem cells (iPSCs), and primary tissues that keep similar functionality of origin tissues [92].

Organoids have been utilized as a 3D *in vitro* tissue structure to understand each tissue's development and disorders. Organoid models have been derived from the liver [93], intestines [94], brain [95], and other tissues. They have been used to understand developmental biology aspects that cannot be directly investigated in animal models. Organoids have also used in drug discovery to resemble the *vivo*-like microenvironment [96]. For instance, the first embryonic liver in vitro organoid was discovered from human-induced progenitor stem cells (iPSCs), mixed with both MSCs and umbilical cord cells (UCCs) in the lab. This organoid could grow and differentiate into liver tissue in the body of mice [93].

In addition, organoids can create from cancerous tissues to recapitulate tumorigenesis in the lab environment. These so-called tumoroids are derived from patients' cancer tissues such as breast [97], colon, and bladder [98]. For instance, in bladder cancer organoids, tissue samples were taken from the bladder tumor and were cultivated as organoids. The research showed that two main growth factors, such as FGF7 and FGF10 were essential to growth of these human bladder cancer organoids. Due to TP53 gene mutation is common in bladder cancer, the MDM2 inhibitor Nutlin-3 was added to the media. As extra Nutlin-3 in cells have a responsibility to induce apoptosis, however in P53 mutation cells, they do not affect cell cycles. Therefore, this test was used to confirm organoids origin is derived from bladder cancer tissue [99].

Further, tumoroids can use as a 3D self-organized platform to evaluate drug efficacy and toxicity in vitro [100].

Spheroids are derived from cancer cell lines or patient's tumor and make self-aggregation on non-attachment plates [101]. Different cancer cell types such as hepatocyte [102], neural [103], breast [104], and lung cancer cells can generate spheroids in *in vitro* [105].

Spheroids and organoids are able to accurately represent the physiological conditions by enabling communication networks between cells. These cell-cell contacts cause ECM proteins secretion, such as collagen, fibronectin, and laminin [106]. Spheroids are formed in 3 steps; first, the integrin of cells surfaces interacting tightly to ECM fibers for making cell aggregation. Second, initial cell aggregation leads to the cadherin expression from the cells and then each cell cadherin binds to neighboring cell cadherin. All of these series steps cause strong cell adhesion and spheroid formation [107]. Cell-ECM interaction can regulate cell migration and adhesion due to integrin activation [108]. The cytoskeleton stabilization and detachment are regulated by talin [28], which has a role in connecting integrin [109] to the cytoskeleton for cell adhesion and migration [110].

Spheroids are formed from outer or proliferative, intermediate or quiescent, and inner or necrotic layers. The level of nutrient, oxygen, and pH are different for each layer. The outer layer of spheroid cells has rapid proliferation due to access to nutrients and oxygen. The intermediate layer has less exposure to soluble factors and oxygen; however, these levels are higher access than the necrotic layer. The gradient level in these three layers makes a different response to cancer drugs. The inner layer of spheroid due to less availability to metabolites and oxygen is faced with hypoxia, low growth rate, or even necrotic cells, and an acidic environment [111]. All of these properties can affect cancer drug response and resistance. It means drug response will be different in each layer of the spheroid. For instance, research on doxorubicin (DOX) drug penetration within multicellular tumor spheroids (MCTs) confocal images revealed that fully drug penetration in outer layer of spheroid after 4 hours of treatment. Meanwhile, no signal of drug was detected in the core of spheroid [112].

The low proliferation rate of cells in the core of spheroids makes them resistant to cancer drugs such as paclitaxel, which stabilizes cytoskeleton microtubules [60]. In addition, cancer drugs like cisplatin and doxorubicin crosslinks DNA and then generation of ROS is secondary effect induced by DNA damage [113]. However, these drugs have less efficacy in a low proliferation rate of cells. So, they do not have high effectiveness and efficiency in the slow proliferation rate of the spheroid core due to *in vivo*-like multicellular architecture [114]. pH gradient is another factor to make anti-cancer drugs inefficient. The cytotoxicity of anti-cancer drugs will reduce the spheroid core in the acidic environment due to reduction of drug penetration into the spheroid [115]. Spheroids reveal strong resistance against chemotherapy drugs compare to 2D cell culture. Therefore, spheroid cultures have been utilized as a tool in tissue engineering for regenerative medicine, tumorigenesis model, and cancer drug testing [116], [117].

Table 1 reviews the properties of *in vitro* 3D cell culture and the difference between 3D scaffold-based and non-scaffold-based cell cultures. 3D non-scaffold-based systems showed more similarity in formation, cellular heterogeneity, gene expression, ECM properties to *in vivo* environment rather than non-scaffold-based systems.

	3D scaffold-based cell cultures	3D non scaffold-based cell cultures
Definition	 Hydrogels Cells are seeded in gel-based 3D structures 	Spheroids Cellular self-aggregation
Cost versus reproducibility	Some materials used to mimic ECM components are expensive (e.g., collagen); Lack of reproducibility.	The majority of the techniques currently used are low cost and allow the production of a large number of spheroids under reproducible conditions
General properties	Cellular heterogeneity: Different cell types may be grown in the hydrogel; Cellular organization within 3D cell cultures occurs spontaneously and can be heterogeneous. Necrotic zones may be formed. ECM: The ECM formed by hydrogels is artificial and may be comprised by only some of the components that are found in the native matrix. Gene expression: Gene expression and cell phenotype are very similar to in vivo tumors. Drug resistance: ECM barriers contribute for resistance to drug Penetration by diffusion	Cellular heterogeneity: Different cell types can be used for spheroids Production. Spheroids have a necrotic core and peripheral layer of cells with a high proliferation rate. ECM: Deposition of ECM occurs in a similar way to that observed in in vivo tumors. Gene expression: Gene expression and phenotype are very similar to in vivo tumors. Drug resistance: The cell-cell interactions and the high density of ECM are responsible for impaired drug penetration.
Commercial products	 3-D Life Biomimetic; Matrigel®; QGel® Matrix; Puramatrix. 	 Low Adhesion Plates; Micropatterned Surfaces (Scivax NanoCulture® multi-well plate); Hanging drop plates (Perfecta3D® and GravityPLUS™ 3D).

Table 1. Properties of in vitro 3D cell culture models.

Table taken from [118]

1.3. <u>Current non-scaffold-based 3D culture systems</u>

Specialized cell culture methods are using to cell aggregation and accumulation a non-scaffold-based system. The structure of these systems allows recapitulating natural cell-cell and cell-ECM interactions to create spheroid and organoid in scaffold free-based models such as hanging drop (HD), ultra-low attachment plates (ULA), magnetic levitation and microfluidic devices [119] (Figure 1. B).

1.3.1. Hanging drop (HD)

Hanging drop system is a type of non-scaffold 3D cell culture that uses open bottom plates that suspend a small amount of media that allows for the creation of spheroids or organoids without cells contact with surfaces. This system uses surface tension at the air-liquid interface to culture cell aggregates inside the media droplet. This media droplet is not big, but the volume is enough to allow for spheroid formation [68]. The advantages of this technique include controlling the spheroid size by adjusting the droplet volume and cell density [120], the fact that it does not need expensive equipment aside from the plates [121], the *vivo*-like environment [122], and evidence of anti-inflammatory and anti-tumorigenic factors secretion [123].

Hanging drop technology applications were found in understanding the cellular and molecular biology in tumor formation and invasion, drug discovery, and tumor cell angiogenesis [124]. In addition, this technology has been used for drug toxicity in hepatocytes. For instance, comparing human liver cancer cell line (HepG2) and primary human hepatocytes (HepaRG) cultivated cells [125] in both hanging drop and 2D cell culture demonstrated high expression of aflatoxin in 3D HepaRG spheroid rather than 2D culture [120].

1.3.2. <u>Ultra-low adhesion plates</u>

Ultra-low attachment (ULA) plates are otherwise standard round or V-shaped bottom cell-culture plates that have been treated with a hydrophilic polymer to inhibit the adhesion of cells [126]. These specific features reduce cell attachment to the plate substrate and promote the self-aggregation of cells and the formation of spheroids like in the hanging drop system. Unsimilar to the hanging drop approach in which spheroid size is limited to the size of the droplet, ULA plates can accommodate the formation of bigger spheroids due to the size of the well of 96 or 384 well plates [127].

Advantages of ULA plates include the fact that there is no need to transfer spheroids to a new plate when they reach a certain size like hanging drop systems. Spheroids were grown in ULA plates, showed tumor microenvironment features like hypoxia, anti-apoptotic and reduce

drug efficacy in patient's breast cancer cells [128]. This system has proven useful in stem cell differentiation, which has used to induce mesenchymal stem cell differentiation similar to the pre-cartilage formation *in vivo* [129]. ULA plates can be helpful for analyzing growth rate and development due to long term cultivation procedures rather than other non-scaffold-based systems [101].

1.3.3. Magnetic levitation

Magnetic levitation system is a new method of non-scaffold 3D cell culture in which cells are mixed with magnetic nanoparticles in a 2D plate. The spheroids are obtained using an external magnetic field on the top of the plate, which aggregate cells by holding them in a stable hanging-drop at the air-liquid interface [130]. The magnetic field is an upward force that helps to counteract geometry, which allows cell-cell interaction and ECM secretion to make spheroid formation [131].

This system can be used to generate spheroids from different tissues and tumor cells in 6 to 384 well plates making it a useful tool for drug discovery and tissue engineering [132]. Spheroids created with the use of magnetic levitation systems have been shown to closely mimic tumor environment. For instance, protein expression of human glioblastoma in vivo was the same as observed in this system [132]. In addition, this system used to assess myeloma stem cells for both niches and drug synergism analysis [68].

1.4. Microfluidic devices

Microfluidic system was introduced as a tool to use as anti-cancer and drug testing in 1990 [133]. Glass and silicon were used as first materials to fabricate microfluidic devices. However, those materials did not provide proper properties such as permeability, compatibility and wettability for these devices (Reviewed in [134]). Recently, PDMS was selected to use as an appropriate material due to having biocompatibility, permeability, transparency, and elasticity [135].

Microfluidic devices use 1-1000 μm-wide microchannels allow for precise control over fluids, drugs, and media in the cell culture system [136]. The control potential of the system involved controlling nutrients [137], and oxygen concentration [138], cell numbers and density [139], cell reproducibility, and tracking of cell growth in a single device [140]. Moreover, the study of gene expression [141], protein secretion [142], and signaling pathways in a single cell have provided in a microfluidic device with a high resolution [143]. Reduced sample size [144], less time consumption, low cost of the experiment, high sensitivity, faster analysis [145], and ease of fabricating are other advantages of this technology to develop biomedical science [146].

This technology has been provided a better 3D cell culture model to mimic *in vivo* microenvironment, such as dynamic, physiological, and biochemical conditions. For instance, lung cells were cultured in the microfluidic devices to recapitulate lung organs *in vitro* by constructing alveolar epithelial cells. The alveolar models have been studied for mechanical stretch influence, intravascular thrombosis, and impact of fluid and solid stress. Recently, this system was considered a reliable model for drug development for Coronavirus (COVID-19) as a global health issue (Reviewed in [147]).

1.5. <u>Differences between 2D and 3D cultures</u>

The first primary method of drug screening is using cell culture. Although 2D adherent cell culture provided much information for scientists and is still widely used in research, it failed to mimic the in vivo cell environment. Cells grown in 2D cell culture have flat morphology and stretched in monolayer with no support of vertical dimension. However, cells in the 3D model have a round shape and aggregating will make a spheroid structure [148].

As well as the rapid proliferation of cells in 2D cell culture, cell lifespan has limitations and is around less than one week. In the 3D cell culture model, cell maintenance takes a long time three weeks, which shows more stability and less proliferation speed [149].

One of the significant differences between 2D and 3D cell culture is cell-cell and cell-ECM interactions. 2D monolayer shows a limitation in contacts, which leads to the absence of niches

in cell populations. However, 3D cell culture provides a proper imitation of cell and extracellular matrix interaction, which can create niches [150].

2D monolayer cell culture often does not lead to the same genes, proteins, mRNA splicing, and topology that exist in the natural cell environment [151]. In contrast, the 3D cell culture model often allows for the similar expression of the genes which are present in vivo [152].

2D cell cultures are more sensitive to drugs rather than 3D cell culture. Because the 2D cell culture model has more access to nutrients and oxygen, which can affect the cell cycle, 3D cell culture model can mimic tumor shape, morphology, and interactions. Therefore, this is to be expected drug response and drug resistance in 3D cell culture is more similar to in vivo. This idea is supported by the research on the MDA-MB-231 breast cancer cell line by using chemotherapeutic agents such as cisplatin and paclitaxel in both 2D and 3D cell culture models. The core of spheroid in the 3D cell culture model showed markedly more resistance to those chemotherapeutic drugs in comparison to 2D cell culture [114]. In addition, test dug toxicity using human hepatocyte HepG2 cells as a liver model in 2D cell culture showed that reducing CYP450 activity is important to drug response and mobility [148]. Therefore, 2D cell culture cannot imitate the natural architecture as in vivo tissue and tumor mass [153].

Section 2. Rationale and objectives

2. Rationale and objectives

2.1. Rationale

Current non-scaffold-based 3D-culture systems such as magnetic levitation, ULA plates, and hanging drop systems are able to make spheroids; however, some limitations arise with these technologies. In the magnetic levitation system, the magnetic field can influence cell behavior [154]. Furthermore, some nanoparticles, such as iron oxide, can color the 3D culture media brown, and therefore influence downstream applications [42]. Also, incomplete attachment of cells to the magnetic nanoparticles can limit the aggregation of cells. Moreover, the magnetic levitation system needs an external magnetic field to aggregate cells, which tends to be expensive equipment [90].

ULA plates are complicated to change media as well as preserving the spheroids. Therefore, new media should be added to the old one on the plates. Besides, the microscopy imaging processes cannot conduct directly in plates and should transfer spheroids to small tubes, which can damage the spheroid shape.

HD culture system has some drawbacks, such as requiring changing the prepared spheroids to non-adherent ULA plates once they reach a certain size. This system is not useful for drug testing because adding the drug in the middle of a small droplet of media and spheroid is difficult. Transferring the HD system is difficult due to the air-liquid interface feature, which could disturb the spheroid shape. In HD system, changing media is impossible and there is no way to take images and do spheroid processing directly in the well [68].

We seek to develop and validate a 3D-printed cell culture system that provides a low-cost and user-friendly method to culture spheroids. This new 3D-printed device, 3D ForCell, contains a media chamber, a microfluidic channel, and a paper-based capillary pump to facilitate media exchange (Figure 2).

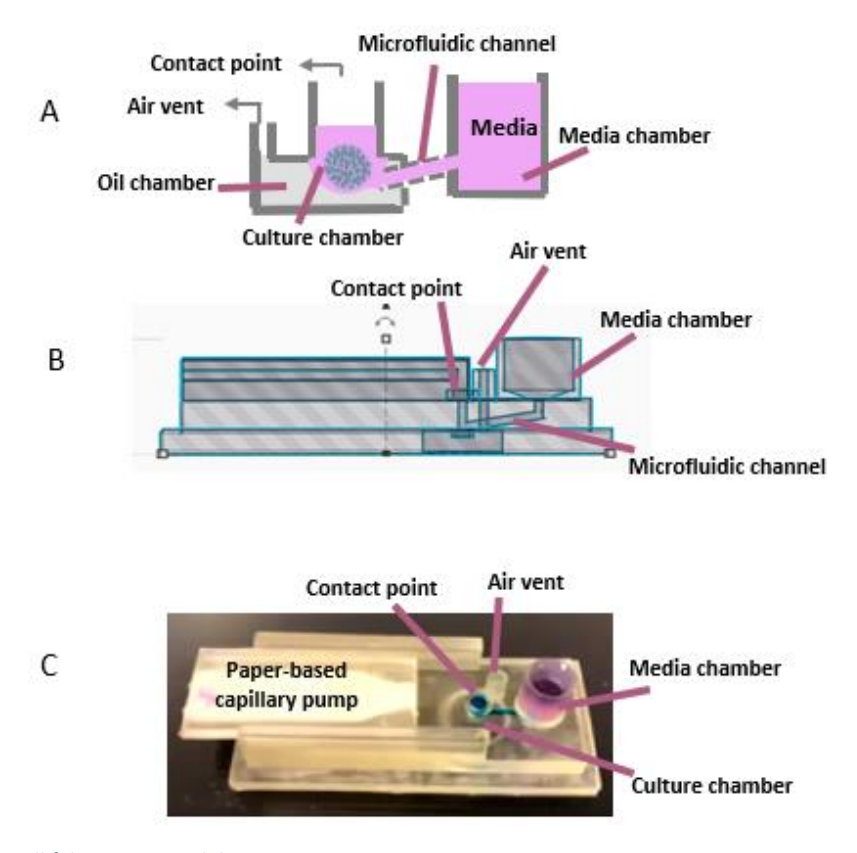


Figure 2. The 3D ForCell fabrication models.

The 3D ForCell 3D printed device with an oil-media interface can make cell aggregation and spheroid formation in the culture chamber. The paper-based capillary pump facilities media exchange.

The culture chamber contains an air vent and uses a media-oil interface to suspend cells and promote aggregation without the usual problems of hanging-drop systems that use a media-air interface. Spheroids are fragile and are thusly hard to transfer for processing and imaging purposes. The 3D ForCell has the potential to use as a single device for processing and imaging. This device also has a paper-based capillary pump to change media. This type of pump has several advantages for the 3D ForCell, such as being low-cost, facile fabrication and disposable. Therefore, this device was designed to resolve the changing media problem in ULA plates and HD systems. The device uses a media-oil interface to suspend cells and promote aggregation without the usual issues of hanging-drop systems using a media-air interface, or the high initial costs associated with magnetic levitation. Spheroids cultured in other systems are fragile and usually hard to process for imaging; the 3D ForCell has the potential to do sample processing

and imaging directly in the device. Altogether, the 3D ForCell platform features are well-suited for real-time analysis to detect biomarkers of interest in response to the prefusion test.

2.2. General objective

The main goal of this research is the development of the 3D ForCell device, so that allows for the growth of spheroids. After getting spheroid inside the device, we would compare these spheroids with those cultivated in a more traditional system such as ULA plates. We also wanted to develop the microfluidic portion of the device, as it would allow a method of media change with minimal impact on the spheroids. We are looking to choose filter paper, which has a slower perfusion rate.

2.3. Specific objectives

 Objective #1 Develop, validate, and qualify the effectiveness of the 3DForCell for spheroid generation and culture.

<u>Objective 1.1</u> Test the effectiveness of the device to produce spheroids.

<u>Objective 1.2</u> Identify the proper filter paper/agarose condition that enables optimal perfusion conditions.

- Objective #2 Compare the spheroids produced in 3DForCell to those produced in ultralow adhesion plates.
 - -Characterize the growth rates of the spheroids in DIC microscopy.
 - -Characterize the spheroids histology (HE and Masson's trichrome; IF/IHC) and set up the protocols [155].

2.4. Hypothesis

This novel device is a better alternative than pre-existing techniques for the generation of the spheroid.

Section 3. Materials and methods

3. Material and methods

3.1. Cell culture

MCF7 (ATCC® HTB-22™) breast cancer cells were cultured in phenol red containing MEM plus 10% FBS, 1% penicillin/streptomycin. A549 (TCC® CCL-185™) non-small-cell lung cancer was cultured in phenol red containing DMEM with high glucose, MEM plus 10% FBS, 1% penicillin/streptomycin, and 1% Glutamax (All reagents from Gibco Canada). Cultivated cells in a plastic flask kept at 37 °C in a humidified atmosphere with 5% CO2.

Media was changed once every 2 days and cells with 70-80% confluency were passaged in a new flask. In short, the media was aspirated with vacuum and cells were detached by a small amount of trypsin 0.05%-EDTA. To do the trypsin inhabitation, an equal amount of media was added to detached cells and centrifuged at 1100 g for 5 min. Cells were counted, and viability was assessed with trypan blue assay.

Cells present in mixture (Number of cells counted)/(Number of squares counted) *(2)(10000)(Volume of cell mixture)

Based on counted cells, the centrifuged cells were suspended in a new media and the desired number of cells were seeded in a new plastic flask and kept at 37 °C in a humidified atmosphere with 5% CO2.

3.2 Fabrication of the devices

Many versions of the 3DForCell design were used over the course of my MSc, but their design and fabrication all followed the same basic process described in Figure 3 and detailed in the following sub-sections.

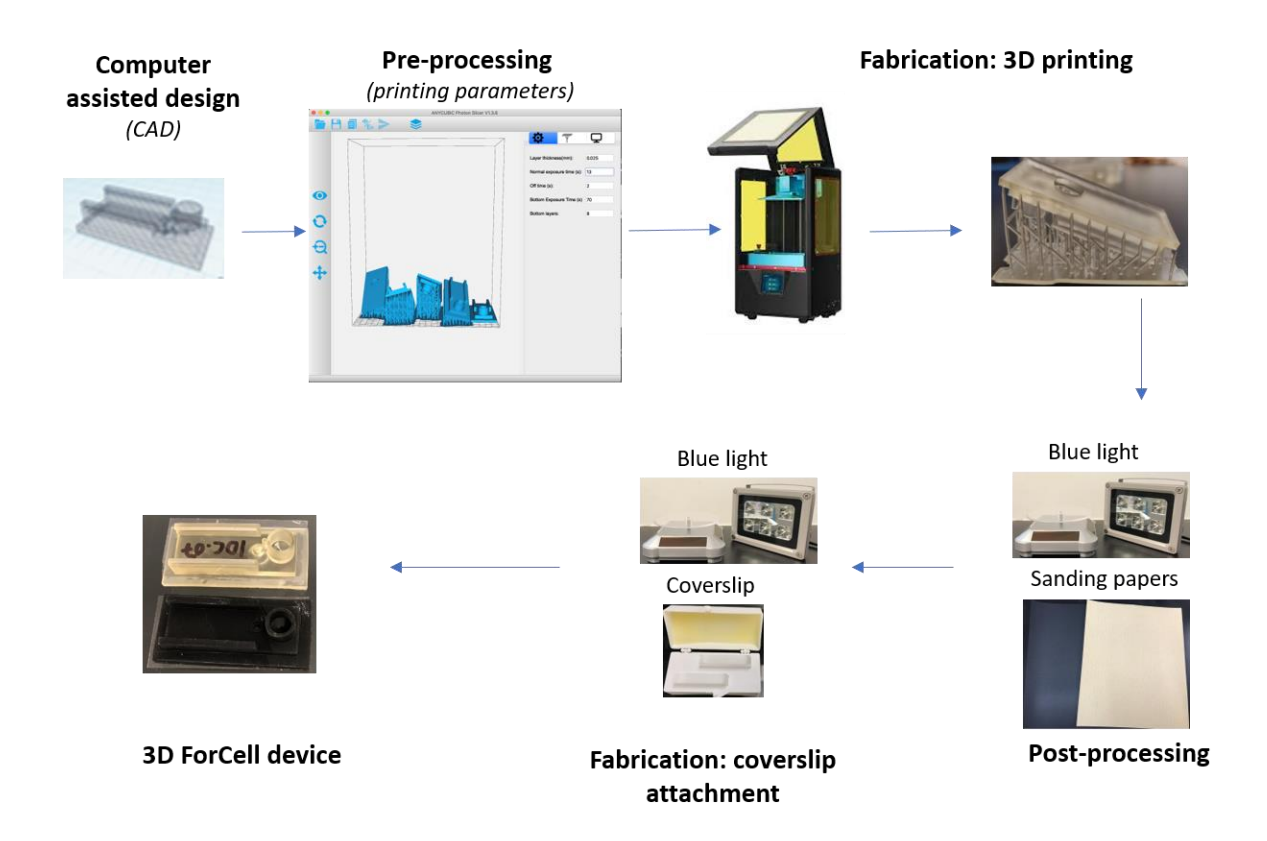


Figure 3. Main steps in the preparation of 3D ForCell devices.

After designing the device in CAD file, different orientations were assessed in pre-processing section. Then devices were fabricated by a LCD-based SLA 3D printer. After that, in post-processing section, they cleaned in 100% EtOH or isopropanol, the supports removed and the resulting device is cured with blue light. Sanding paper was then used to make the surface of the bottom smooth. The coverslip was prepared to stick in the bottom of the device and blue light was used to cure glue or resin and make them harden. Finally, the 3D ForCell device is ready to use.

3.1.1. <u>Computer-assisted design (CAD)</u>

All versions followed the same basic design (Figure 2. B), albeit with slight variations in terms of size or composition (Figure 4) and (Table 2). All 3D models were created using Solidworks (Solidworks, Dassault systems), a 3-dimensional computer assisted design program.

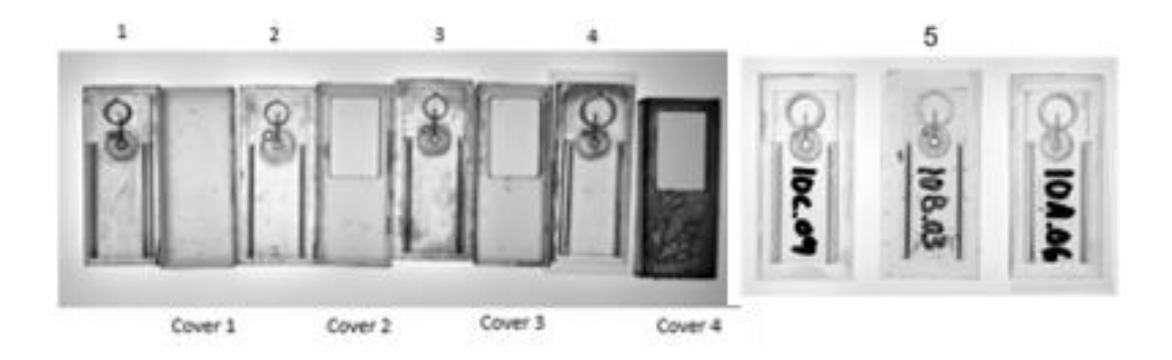


Figure 4.Different versions of 3D ForCell devices.

Whole of device development reached to print 5 versions of devices. In version 5 of 3D ForCell device, 3 models with different culture chambers size were fabricated.

	Version 1	Version 2	Version 3	Version 4	Version 5
Frame size	Height: 110 mm Width: 35 mm	Height: 110 mm Width: 35 mm	Height: 110 mm Width: 35 mm	Height: 110 mm Width: 35 mm	Height: 120 mm Width: 40 mm
Media chamber size	Diameter: 9 mm Height: 10 mm	Diameter: 9 mm Height: 10 mm	Diameter: 9 mm Height: 10 mm	Diameter:12mm Height: 10 mm	Diameter:15mm Height: 10 mm
Air vent size	Diameter: 2 mm Height: 1 mm	Diameter: 3 mm Height: 2 mm	Diameter: 3 mm Height: 1 mm	Diameter: 3 mm Height: 1 mm	Diameter: 3 mm Height: 1 mm
Bottom thickness	3 mm	2 mm	2 mm	2 mm	2 mm
Media chamber wall thickness	1 mm	1 mm	1 mm	1 mm	2 mm
Culture chamber wall thickness	2 mm	2 mm	2 mm	2 mm	3 mm

Table 2. Size variation in composition of the 3D ForCell device versions.

All models have the same overall components contained a media chamber to facilitate media exchange, a microfluidic channel, a culture chamber, an air vent, and a paper-based capillary pump (Figure 2. A, C). Each part of the device was designed to fill a specific function. The microfluidic channel is placed between media and culture chamber to transfer media from media to culture chamber. The air vent is placed near the culture chamber to remove air from the oil chamber; meanwhile, the oil is added to the device's oil chamber. The paper-based capillary pump can change media when touched contact point in top of the culture chamber.

3.2.1 Pre-processing (printing parameters)

These models were then imported into Anycubic 3Dprinter software to set up parameters such as slicing, exposure time, printing angle, and the use of temporary supports. 3D models must be virtually "sliced" into individual 2D images; because the printer can only print one at the time. The printing angle is critical to the success and quality of the final product as 3D printing does not allow for hanging portions (i.e., it is impossible to print structures not attached to anything). The use of temporary supports can add a bit more flexibility; however, the use of supports also needs to be optimized and their removal comes with its own set of challenges. Optimization of the printing angle and temporary support is deeply model-dependent and is the subject of section 4.3.3.2.

3.2.2 3D printing

3D printers create objects layers by layers by adding material directly or by polymerizing material such as UV-curable resin. This can be done indirectly via a LED placed behind an LCD screen/mask (MSLA) (Figure 5. A), directly via passing back and forth a laser inside a vat of photocurable resin (laser-based SLA or LSLA) (Figure 5. B) or by projecting images via direct projection (DLP-SLA) (Figure 5. C).

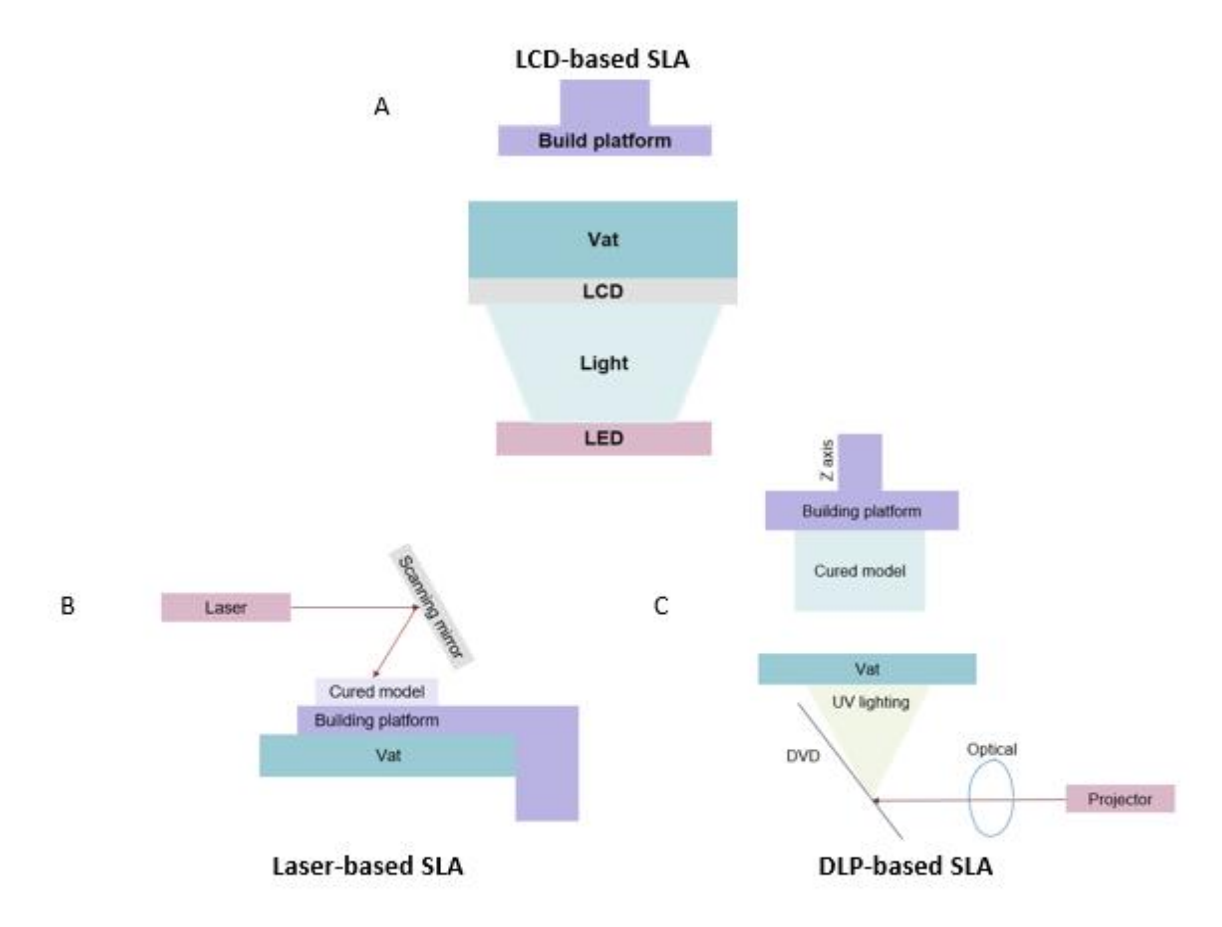


Figure 5. All 3D printer models.

There are 3 main 3D printers, such as LCD-based SLA, laser-based SLA, and DLP-based SLA. In both LCD and DLP the source of light is at the bottom of device to cure the resin; however, the LCD used LED light and DLP used a digital light projector to solidified the resin. In laser SLA 3d printer the source of light is a laser on the top of device and there is a mirror to adjust laser beam.

All of my devices were printed using UV-curable resins (Anycubic, transparent, black; Eleegoo, transparent) and a desktop LCD-based SLA 3D printer from Anycubic, Photon (Figure 6).



Figure 6. Anycubic photon LCD-based SLA 3D printer.

These images showed that the type of LCD-based 3D printer, which was used to print the 3D ForCell device. Image taken from [156].

3.2.3 <u>Post-processing</u>

After printing is complete, the devices were removed from the printing platform and were washed with 100% ethanol or 100% isopropanol to remove the excess and unpolymerized resin. Temporary supports were then removed, and the devices were immersed again in 100% ethanol or 100% isopropanol and washed for 5 min with the help of a magnetic stirrer.

Remains of the temporary supports and imperfections were then removed by the careful use of sanding papers (grade 320, 400, and 600). Printing parameters and tilt of the model were always optimized in order to minimize sanding.

Finally, devices were sealed with the use of coverslips (optical plastic or glass type), which were stuck to the bottom of device with UV-curable glue or resin (the same one used for the devices). A UV source or LED blue light was used to cure the glue or resin in coverslip.

3.3 Leak test of 3D ForCell devices

The oil chamber was first loaded with oil. Media well was then filled with media, which also loaded the culture chamber (Figure 7). Devices were kept at 37 °C in a humidified atmosphere with 5% CO2 for 2 days. Images from devices were taken by an imager in day 0 and day 2 after the experiment. Devices that were obviously leaking were not used in subsequent experiments.

3.4 Spheroid production

3.4.1 <u>Ultra-low adhesion plates</u>

The MCF7 and A549 cells were seeded in mammosphere media consisting of DMEM/F12 containing B27 supplement, 5μg/ml insulin, 20 ng/ml recombinant epidermal growth factor (EGF), and 10ng/ml Basic fibroblast growth factor (bFGF) (all reagents from Gibco Canada). Spheroids were produced using a previously established protocol based on the method described in [157, 158]. Briefly, cells were first detached by using trypsin-EDTA at 70-80% confluency and centrifuged at 1100 g for 5 min. After removing the supernatant, cells were suspended in 1-5 ml of culture media and passed through a 25G needle. Uniformity of the cell suspension and its concentration was assessed using a hemocytometer. Cells were diluted in mammosphere media at appropriate density which were 500 cells/ml for MCF7 and 250 cells/ml for A549 [159], [160].

100uL of either cell suspension was then used to seed ULA plates, which served as a positive control in all experiments. Plates were incubated, humidified atmosphere at 37 $^{\circ}$ C with 5% CO2 for minimum 5 days for ULA plate during plates were incubated without moving or disturbing the plates, and without replenishing the media before the 5 days mark after wise media was replenished via the addition of 50 μ l of mammosphere media/well.

3.4.2 3D ForCell

Devices were seeded using the following approach. First, oil was added (100 μ l) from the culture chamber, with the help of a loading tip. Then diluted cells were added using one of two protocols. In the first approach, diluted cells were seeded via the microfluidic channel, which allowed them to reach the culture chamber (Figure 7. A). After that, media was added (200 μ l) to the media well. In the second seeding protocol, cells were seeded directly from the top of the culture chamber (Figure 7. B). The media was then added to the media well. In either case, once seeded devices were put in the incubator. Every 2 days, the old media was removed, and fresh media was replaced in the device.

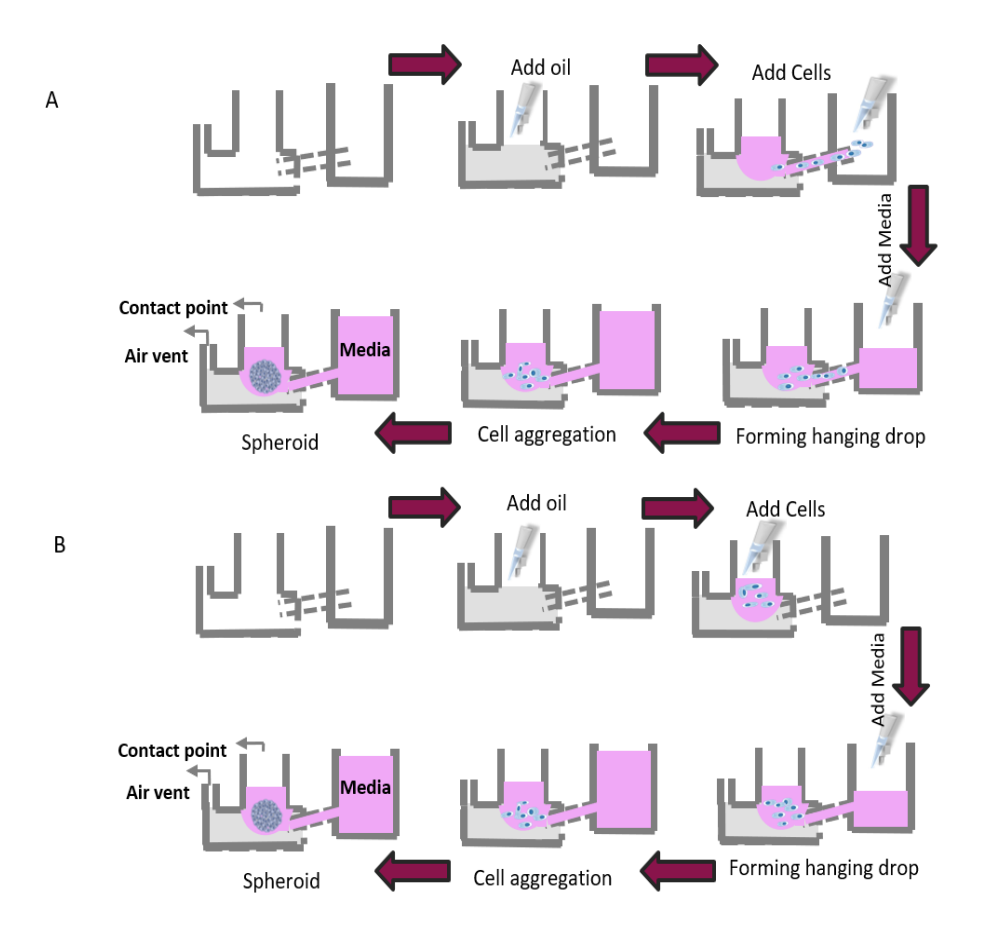


Figure 7. Cell seeding from the media chamber and the top of culture chamber.

A)100 μ l of oil was added from the top of culture chamber, then desired density of diluted cells was added from the top of culture chamber. Media was added from the media chamber, forming a hanging drop. The cells aggregated in the culture chamber and spheroid formed after at least 5 days of cell seeding. B) 100 μ l of oil was added from the top of culture chamber, then desired density of diluted cells was added from the media chamber. Media was added from the media chamber and cells reached to culture chamber through microfluidic channel forming hanging drop. The cells aggregated in the culture chamber and spheroid formed after at least 5 days of cell seeding.

3.5 Sterilization procedures

In the first sterilization protocol, devices were put in 50 ml 70% of ethanol falcon for 5 min. Then devices were kept under BSC to dry up.

In the second sterilization protocol, devices were put under UV light of a clean BSC cabinet for 15 minutes. Then PBS (1x)/ 1% penicillin/streptomycin (PS) was added to both culture and

media chamber for 15 minutes (All reagents from Gibco Canada). Then, devices were kept under BSC to dry up completely.

3.6 Spheroid growth measurement

The number of spheroids with a ≥50 µm diameter were counted after 5 days via the DIC microscope for both the 3D ForCell device and ULA plates. Mammosphere forming efficiency (MFE%) was also assessed using the following formula:

MFE % = number of mammospheres per well/ number of cells seeded per well *100
We also measured the diameter of spheroids by using eyepiece graticule and DIC microscopy
[160].

3.7 <u>Processing of spheroid for whole-mount immunofluorescence microscope</u>

3.7.1 *Fixation*

Spheroids (100-200 µm in diameter) were transferred to the fixative solution, which contained PBS, 4% PAF, 0.1% glutaraldehyde and phalloidin, for 1h at room temperature. Cells were washed one time by PBS and incubated for 1h at room temperature. Blocking and permeabilization consisted of incubation in blocking buffer containing PBS 0.1% Triton, 10% BSA fraction V and 0.02% sodium azide at 4°C for 2 days. Spheroids were then washed in PBS plus 0.1% Triton x100 (All reagents from Gibco Canada).

3.7.2 OCT mounting

Spheroids (100-200 μ m in diameter) were transferred in 50% OCT. Then spheroids were transferred from 50% to 75% OCT. Immediately, after 75% OCT, spheroids were transferred in 100% OCT. To make an easier track while sectioning by microtome, 10 μ l of food color was added to spheroid tubes. The spheroids suspended in OCT were then quickly frozen the spheroid by placing them on dry ice. The samples were kept at -80 °C until ready for cutting.

3.7.3 Hematoxylin and Eosin (HE) staining

After spheroid sectioning by microtome, 8 µm thick sections were placed onto glass slides. Cytosol (Fisher scientific Canada) was used to clear and deparaffinized the samples. Then ethanol was used in different concentrations to rehydrate the samples. Based on routine protocol [161], [162], the slides were dipped 10 times in milli Q water then they were stained by Mayer's hematoxylin (Sigma Canada). After hematoxylin staining, slides were put indirectly under running tap water. The slides were dipped 10 times in milli Q water and after that, slides were dipped 10 times in ethanol 95%. The slides were stained by eosin Y solution 0.25% (Sigma Canada). Ethanol was used in 95% and 100% concentrations and then Cytosol was used for the prepared slides. Finally, the slides were mounted with coverslips and were dried under the fume hood for 48 hrs.

3.7.4 <u>Live-microscopy Staining</u>

CellTracker™ orange-CMRA Stain (Invitrogen) was used to label the cell's organelles to monitor cell movement, migration, and proliferation in the 3D ForCell device with a UV laser. The stock source was prepared to a working concentration (1000x) 10 µM in a serum-free medium. After warming the CellTracker™ working solution to 37°C, it was added to the media chamber of 3D ForCell device and ULA plates. Both devices and plates were incubated 15-45 minutes in a humidified atmosphere at 37 °C with 5% CO2. The dye was removed from the cells and fresh media was added to wells.

Cell mask green plasma membrane stain (Invitrogen) was used to label the plasma membrane to track cell-growth/spheroid formation in the 3D ForCell device. After preparing the working dilution of the cell mask (1X), it was kept at 37°C to warm up. The media was removed from wells in both plates, 3D ForCell device, and the working dilution were added to wells. It was

incubated for 1 hr at an incubator. Then, the staining solution was removed and new media was added to each well.

3.8 Capillary pump.

To do perfusion tests, different thickness of the Whatman filter papers (grade 1: 180 μm, grade 2: 190 μm, grade 3: 390 μm, grade 5: 200 μm) were put on a cassette strip (Figure 8).



Figure 8. Cassette strip with filter paper.

This type of cassette by using filter paper was used to do perfusion test.

3D ForCell device was loaded based on the procedure described in section 3.4.2. The cassette and loaded device were both weighted with a laboratory balance (Sartorius company of Germany) before the experiment. Timer was started as soon as the filter paper makes contact with the culture chamber. Timer was stopped whenever the filter paper was filled. The cassette with filter paper was removed, both cassette and device without cassette were weighted by balance. The perfusion rate was assessed by measuring the media weight (mg) at various time (second) intervals for all the cassettes types. Figure 9 showed that how the paper-based capillary pump can change the media for the 3D ForCell device.







Figure 9. Steps of changing media with a paper-based capillary pump.

A)For changing media the filter paper touched the contact point at the top of the culture chamber. B) this image showed that the pink color media absorbed until the middle of the filter paper. C) Whole the filter paper filled from media completely.

The same experiment has done for all models of version 5 to assess culture chamber size can affect the perfusion test. In addition, the filter papers flow rate was tested in this experiment for all of version 5- a, b, and c models.

3.9 Imaging

DIC images were taken with an Axiovert 200 DIC disk on a Carl Zeiss inverted microscope and EM-CCD cameras. Images acquisition was performed with Northern Eclipse. Cells seeded in devices were kept at 37°C with 5% CO2 using this microscope with 10X objective to confirm they are in good condition and evaluate their proliferate and growth.

Section 4. Research findings

4 Research findings

4.1 3DForCell version 1.0

Version 1 of 3D ForCell device was fabricated by a photon LCD SLA 3D printer (Figure 10). The frame version 1 was 110 mm long and 35 mm wide. The oil chamber had a 190-200 μ l capacity and the media chamber had a 100 μ l capacity. The air vent with 2 mm in height and 1 mm diameter was used to remove bubbles from the oil in the oil chamber. The media chamber has 9 mm diameter and 10 mm in height. Due to having a high capacity in the oil chamber, it had a high thickness of around 3 mm.

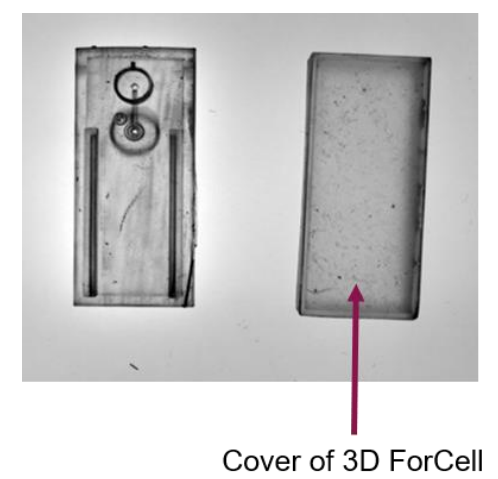


Figure 10. The 3DForCell version 1.

Version 1 of 3D ForCell device with cover was fabricated in 6 replicates.

After 48 hours of seeding cells in 6 devices, 4 devices dried up completely and 2 others did not have any media. Therefore, we could not see any spheroids. We stopped cell cultivation and modified the design of the device.

Potential source of problems: The oil came out from air vent when we added cells to the media chamber and made more challenges during cell seeding. The device's initial concept included a cover that needed to be removed before imaging under bright field microscope, needlessly complicating the process. We quickly found out that the thickness of the oil chamber made observations difficult and supposed that the same problem would be worst when we moved to

confocal microscopy. Because of some problems in the design of device, we moved to version 2.0.

4.2 3DForCell version 2.0

In version 2, the frame of the device was printed the same as the first version (Figure 11. A). The media chamber size was printed the same size of version 1. The size of the air vent increased with 3 mm height and 2 mm diameter, to prevent oil and media leaking out. The bottom thickness of device changed from 3 mm to 2 mm (Figure 11. B). Removing the cover of device and transferring it to the petri dish to observe device under the microscope made daily observations difficult. As such, we modified the cover design to include a window that allows for observation without the need to transfer into a petri dish. The new cover used the same transparent optical-grade plastic used at the bottom of device. However, we did not use the second version of device to cultivate spheroids as the larger vent did not allow for the use of the perfusion cassette.

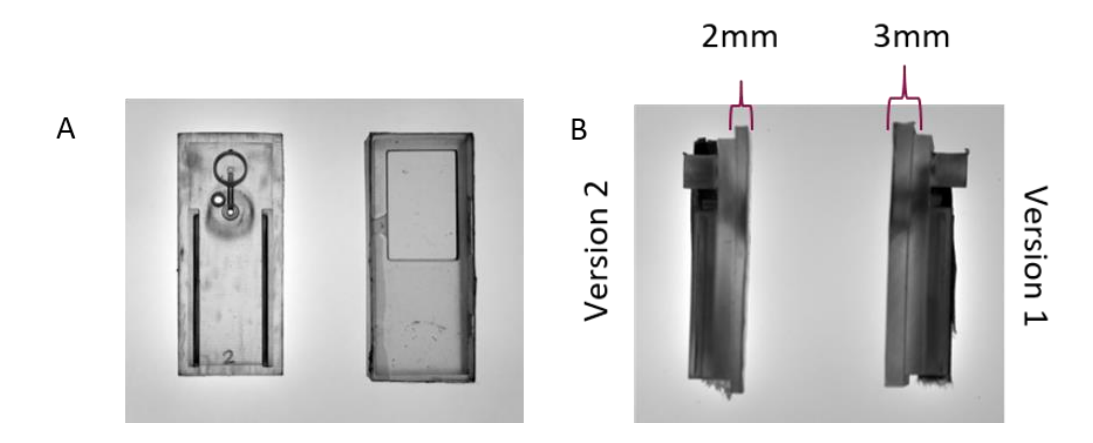


Figure 11. 3D ForCell device version 2.

A) These images showed version 2 of 3D ForCell device which printed with bigger air vent. B) The difference between the thickness of version 1 and 2 of 3D ForCell device is obviously demonstrated in section B.

Potential source of problems: In this version, the larger vent (Figure 11. A) resolved the oil leakage issue from the air vent, it also prevented the effective use of the perfusion cassette.

4.3 3DForCell version 3.0

In the third version, the frame size of device, culture and media chamber size were the same as version 2. However, the air vent size was reduced so that it was smaller than the one from version 2, but bigger than version 1, 3 mm height and 1 mm diameter (Figure 12). This change allowed efficient perfusion while also solving some of the oil-leakage issue we had in version 1.



Figure 12. 3D ForCell version 3.

Version 3 of 3D ForCell device was fabricated with a smaller air vent in comparison of version and bigger than version 1.

We then proceeded to seed the devices to assess spheroid formation. A total of 18 devices were seeded in the course of 3 separate experiments. In the first 6 devices, most of the media and some of the oil disappeared from the culture chamber and the media chamber after 48 hrs of culture. No spheroids or cells could be observed in these devices. As such, in the next experiments, we tried to minimize evaporation by putting sterile, PBS-soaked swabs in the place of the cassette and the dishes containing the devices. Despite this, most of the devices lost either their media, oil, or both and all both were completely dry after 5 days, despite adding media every day. From 18 replicates version 3, 14 of devices had leakage issues. The oil used in the device has a very high evaporation point (200°C) and the incubator and 100% humidity. Therefore, the problem was likely not to be evaporation. After taking a closer look at the devices and found some cracks in the devices themselves, and under the plastic coverslip (Figure 13).

Before experiment After experiment

Figure 13. Cracks presented in the 3D ForCell device.

The image compared 3D ForCell device before and after the experiment. After 3 days of experiment, several cracks appeared on top, bottom, and microfluidic channels of the device.

Potential source of problems: Ethanol 70% sterilization may have been responsible for the cracks, has untreated devices did not have these defects. Furthermore, incubating them at 37°C made this effect stronger. It is, therefore, likely that media, oil, or both leaked from their chamber and into the cracks or out to the petri dish.

4.3.1 Effect of ethanol and long-term ethanol incubation on devices

We wanted to know what was the source of the cracks: ethanol or device incubation. We selected 1 device to sterilize with ethanol 70% and kept in incubator and 2 others without sterilization. One was left at room temperature and another in incubator. After 24 hrs, we checked those devices; we could not see any media after 1 day in the sterilized device (Figure 14). While EtOH is used in post-processing, we still modified our sterilization protocol (section 3.5) to minimize the exposure of the finalized device to EtOH, as the glue used to hold the coverslip may not entirely be compatible with 70% EtOH exposure.

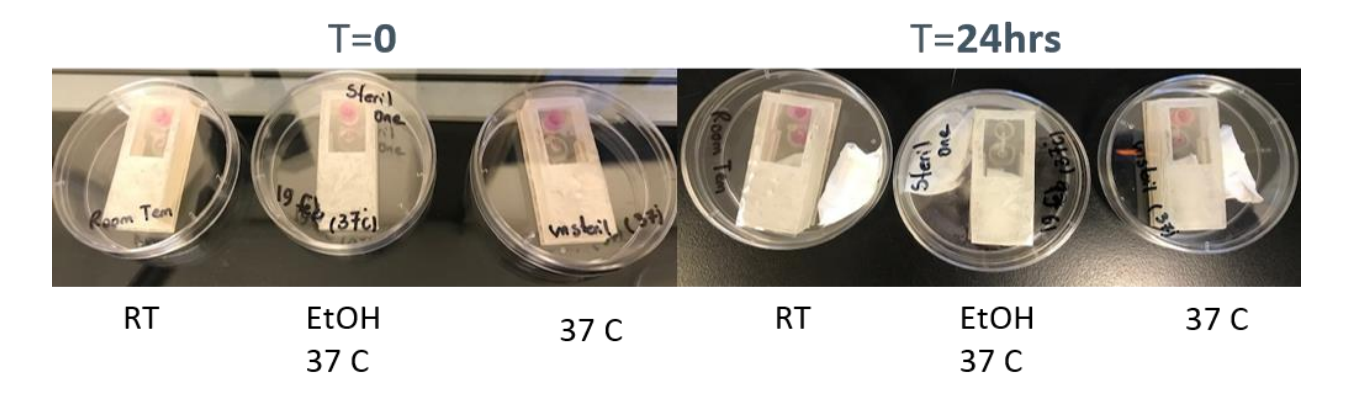
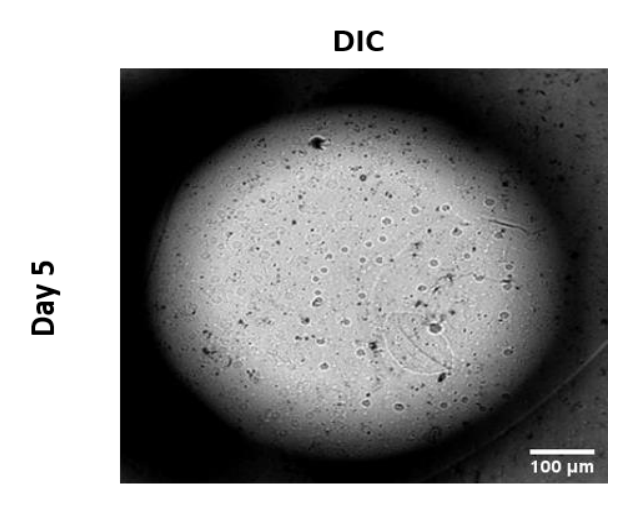


Figure 14. Test sterlization protocol.

Two sterilization devices were kept in room temperature 37C and one sterilization device was kept at room temperature. Their changes were evaluated after 48 hrs.

4.3.2 Test 3D ForCell version 3 cell seeding, No spheroid?

We tried to cultivate cells on 4 left intact devices of version 3, to check the new sterilization protocol. The devices were sterilized with UV and PBS/PS and then cells were added to devices from the media chamber, with the assumption that cells will reach to culture chamber through the microfluidic channel. After 5 days of incubation, we could not see any spheroid in the device, as shown in figure 15.



A549 Device

Figure 15. Cell seeding attempt in version 3.

This image showed that there is no A549 spheroid in the 3D ForCell device after 5 days of cell seeding.

Because the absence of spheroids in our devices could also be attributed to our cells themselves, we assessed the spheroid potential of our two model cell lines using ULA plates, as well as our devices. Figure 16 showed that A549 and MCF7 spheroids could grow in ULA plates. However, there is no spheroid in devices after 5,10 and even 15 days.

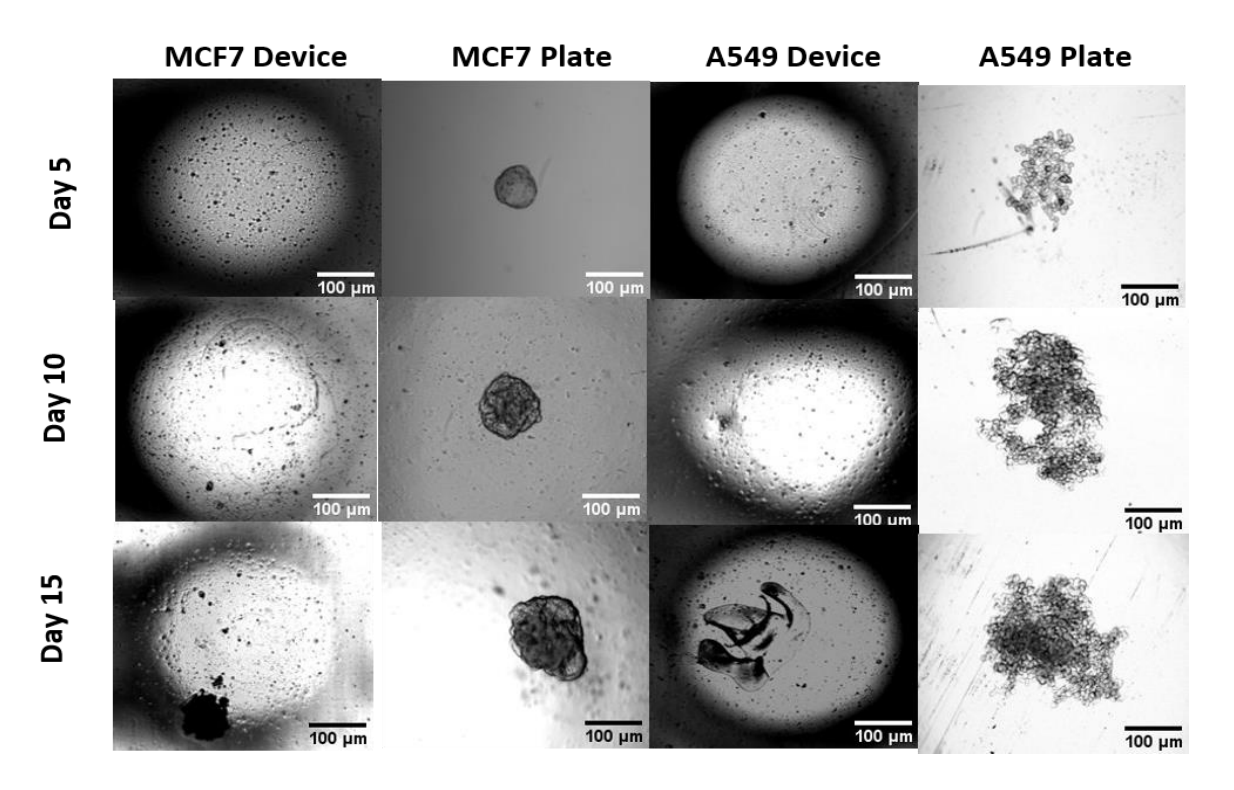


Figure 16. Compare 3D ForCell device and ULA plates.

3D ForCell devices version 3 could not grow the spheroid, but A549 and MCF7 are clearly present in the ULA plates.

For making sure those generated spheroids in ULA plates were able to secrete matrix, we prepared H&E staining slides. These slides were prepared from MCF7 spheroid in day 5/10/15 after cell seeding (Figure 17). We could set up producing and H&E staining protocols for spheroid in our lab.

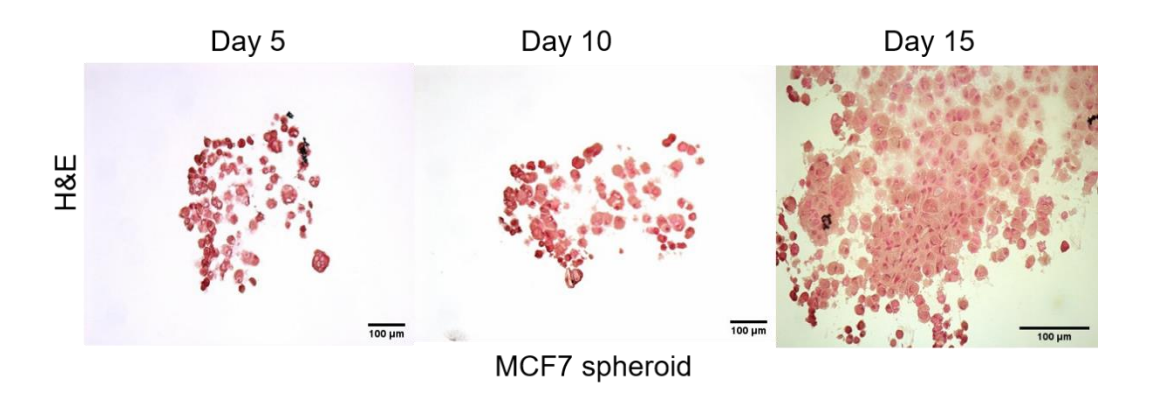


Figure 17. H&E staining images from MCF7 spheroid.
These H&E slides prepared from MCF7 spheroids that generated in ULA plates. The images showed that these spheroids were able to secrete the matrix around themselves.

After confirming the spheroid protocol and making sure no spheroid has appeared in 3D ForCell devices, we used the cell mask to check is there any cells in the culture chamber of devices. We compared result of the cell mask in the device with ULA plates. We had MCF7 spheroid in ULA plates, but we could not detect any signal of cells in the culture chamber of 3D ForCell devices after 5 days (Figure 18).

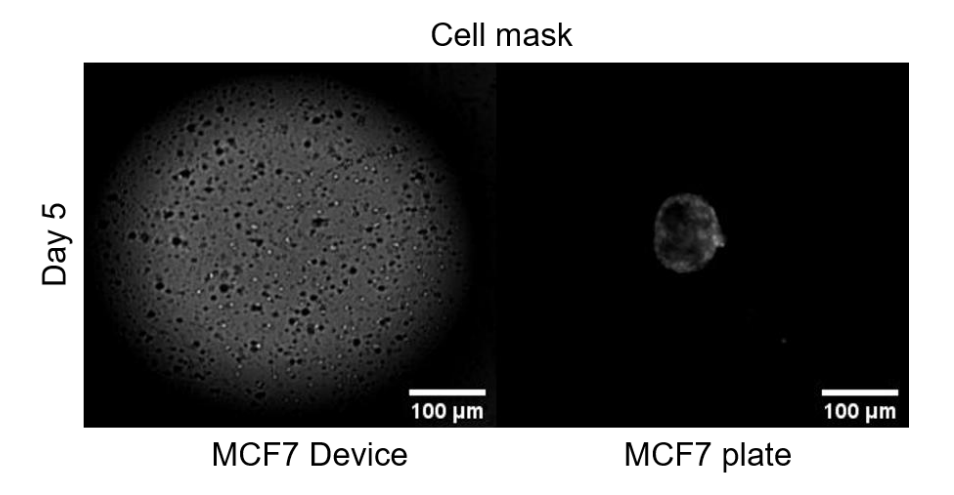


Figure 18. Fluorescence labeling.

Cell mask was used to label cells in both the 3D ForCell device and the ULA plates. No signal detected from the device, but MCF7 spheroid is present in the ULA plates.

Potential source of problems: Because there were no cells in the culture chamber of 3D ForCell device after using the cell mask, we proposed that maybe the problem is the way of cell seeding. We assumed that maybe the cells could not reach the culture chamber and they just remained in the microfluidic channel. Therefore, we decided to seed cells from the top of the culture chamber in our next attempt.

4.3.3 3DForCell version 4.0

In version 4, we increased the media chamber to 12 mm in diameter, from 9 mm that was used in previous versions. The new media chamber has 200 μ l capacity as the previous version had 100 μ l volume capacity. Increasing the size of the media chamber was a good idea to minimize the negative effect of media leakage issues by increasing the media volume. We replaced glass coverslip instead of an optical plastic coverslip (Figure 19). This replacement was because some cracks appeared on an optical plastic coverslip after around 2 days of cell seeding. In addition, glass coverslip was more convenient for cell observation and imaging. The plastic adhesive was replaced by a UV-curable glue in order to stick the glass coverslip to the bottom of the device.

Because we want to make sure the glass coverslip sticks entirely and there is no hole to allow oil/ media leakage.



Figure 19. 3D ForCell device version 4.

Version 4 of the 3D ForCell device was printed with a bigger media chamber. The glass coverslip used for the bottom of device and UV glue was steaked coverslip to the device.

8 replicates of devices were printed and 4 of them had leakage problems when they were tested without cells. In the devices that leaked, the oil and media leaked between glass coverslip and devices. Those 4 devices were removed from the rest of the experiments.

4 devices were tested without cells after sterilization with a new method without using ethanol. Because we wanted to check is there any leakage issue arises with a new sterilization protocol. Then, they were kept at incubator for 2 days. After 2 days, there was oil/ media leakage in 2 of those devices, but 2 others worked completely fine without any leakage issue (Figure 20).

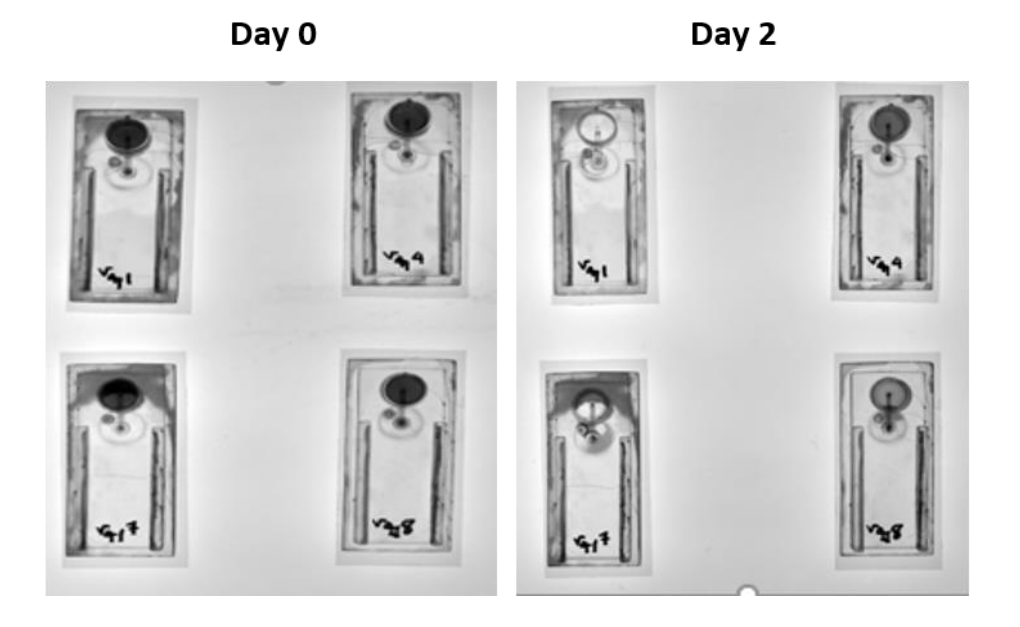
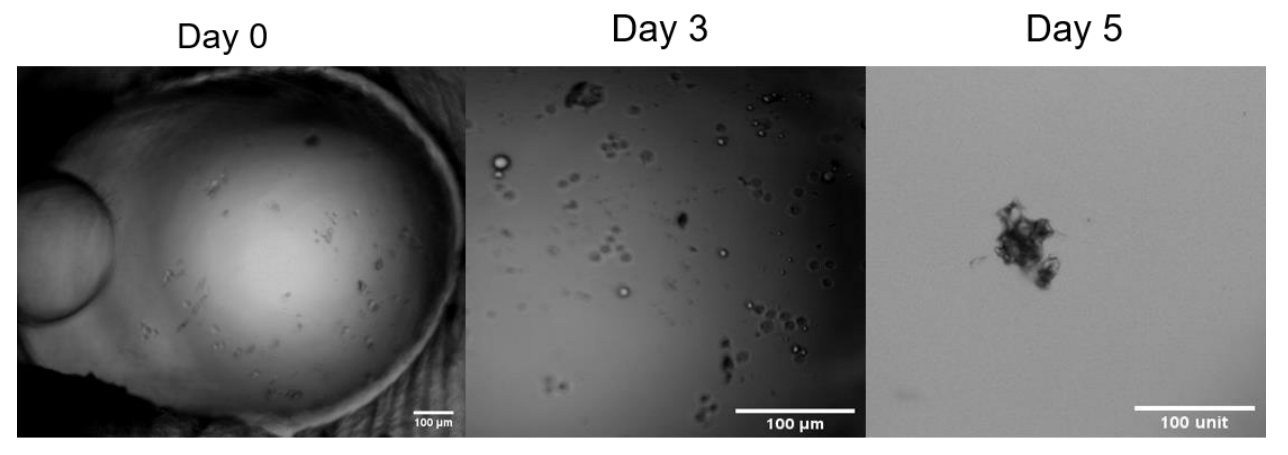


Figure 20. Test the 3D ForCell device version 4 without cells. From 4 of 3D ForCell devices version 4, all of them did not have an oil leakage problem, but 2 of them could not keep media after 2 days.

Potential source of problems: As a gray color appeared on the surface of 2 devices in day 0 showed that those devices defected before the experiment. Maybe the way of device fabrication or UV glue did not have good quality and it causes media leakage problems after 2 days.

4.3.3.1 Cell seeding from top of culture chamber in 3D ForCell version 4.0

We selected 1 of those 2 devices that did not have media leakage problem. Images were taken from the culture chamber of the device in day 0 and day 3 showed that several cells are present in the culture chamber (Figure 21), contrary to the situation seen in figure 16. After day 5, a small spheroid might have formed in our device, as can be seen in figure 21. The image showed that it looks similar to A549 spheroid that we had in ULA plates in figure 16. In addition, it appeared in the timeline we expected for spheroid formation.



A549 Device v4.0

Figure 21. Spheroids growing in 3D ForCell v4.0.

Seeding the cells from the top of the culture chamber in the 3D ForCell device version 4. In day 0 and 3 can see some cells in the culture chamber of 3D For Cell device. On day 5, a small spheroid formed in the culture chamber of device version 4.

To have a bigger size of spheroid and remove the media leakage problem, it is better to find some solutions to improve version 4 of 3D ForCell device.

4.3.3.2 <u>Can we improve 3D ForCell fabrication?</u>

We decided to shift some of our focus on improving our pre-processing, fabrication, and post-processing methodology based on the first success. SLA-based 3D printing, while more flexible than filament-based 3D printing, still has problems printing overhangs. These include layers needing to rest on a previously printed portion of the object; by temporary support structures. Most 3D printing guides [163] indicate that a good rule of thumb is to find a model orientation in which most structures are below 45° from the perpendicular of the plate. Given a complex model is not always straightforward and even possible way. Because finding the best printing orientation can be tricky as the best orientation may lead to on very long printing time (increased number of layers when an approach is a perpendicular). As such, we tested various printing parameters in order to minimize the use of support (requiring sanding) while

diminishing print time. The use of support could also damages the model as they need to be sanded away. While sanding may provide a better surface for the coverslip, this was never directly assessed. In addition, we assumed that the leakage problem could be due to the fact that our initial post-processing protocol used natural light to finish curing the device. This is far from ideal and may have led to unpolymerized components in the device, which may even be the main reason for some of our leakage issues. Therefore, we modified our post-processing protocol to include better sources of 405 nm light, such as UV source of an imager and a commercially available blue light instead of natural light or the pen-light shipping with the UV-curable glue we used to mate glass coverslips the last set of devices.

Device number	Sanding	Coverslip	Adhesive	Curing	Result
4.9	Full (320-600)	Glass	Glue	Pen	Leakage media
4.10	Full (320-600)	Glass	Glue	Imager	OK
4.11	Full (320-600)	Glass	Glue	Pen+ Imager	OK
4.12	Full (320-600)	Glass	Glue	Imager	OK
4.14	None	Glass	Glue	Pen	Leakage media
4.17	600	Glass	Glue	Imager	OK
4.18	None	Glass	Glue	Pen+ Imager	Leaking media
4.21	None	Glass	Resin	Imager	Leaking media
4.22	600	Glass	Resin	Imager	OK

Table 3. Examples of the post-processing conditions tested.

By varying the printing angles and changing the curing protocol, we were able to significantly improve the overall quality of the print and reduce our leakage problems (Table 3). While some orientations required sanding of the bottom surface before use, the use of sanding papers after printing 3D was not detrimental as reduced possible oil/media leakage issue. These orientations had the added benefit of minimizing overhangs of the cassette supports. Exposing printed devices to UV of the LED pen was not sufficient to polymerize the monomer's components of resin material and UV-glue due to having leakage problems (Table 3).

4.3.4 3DForCell version 5.0

To improve media leakage issue, we moved to version 5. In a new version, we used a bigger frame for devices. The height of device in version 4 was 110 mm and it was changed to 120 mm in version 5. The width of the device in version 4 is 35 mm and it changed to 40 mm for the new version. We made the frame of device bigger rather than previous versions so that it is closer to the size of the coverslip. Increasing the size of the frame helps cover glass coverslip more than before and prevent it from shrinking.

The media chamber and culture chamber wall thickness have changed from 1 mm and 2 mm to 2 mm and 3 mm in version 5. We used high thickness in the wall chambers of this version to make printing easier (Figure 22).

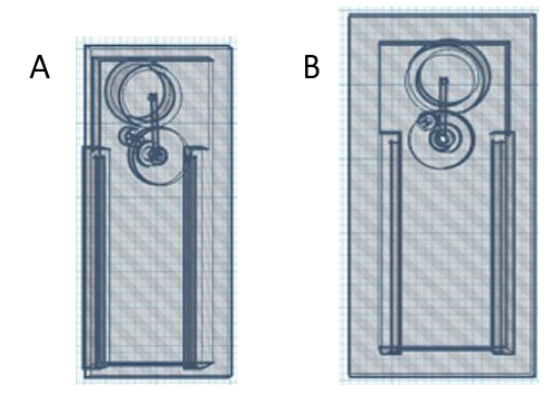


Figure 22. Compared version 4 and 5 of the 3D ForCell.

A)The height of version 4 is 110 mm and the width is 35 mm. The media and culture chambers wall thickness was 1 mm and 2 mm. B) The height of version 5 is 120 mm and width is 40 mm. The media and culture chamber's thickness changed to 2 mm and 3 mm. In version 5, we increased the culture chamber size from a to c with seeding different cell densities. Therefore, we can compare which one will provide a better result. The different sizes in the culture chamber of model a to c are present in figure 24.

In version 5, we increased the culture chamber size from a to c (Figure 23).

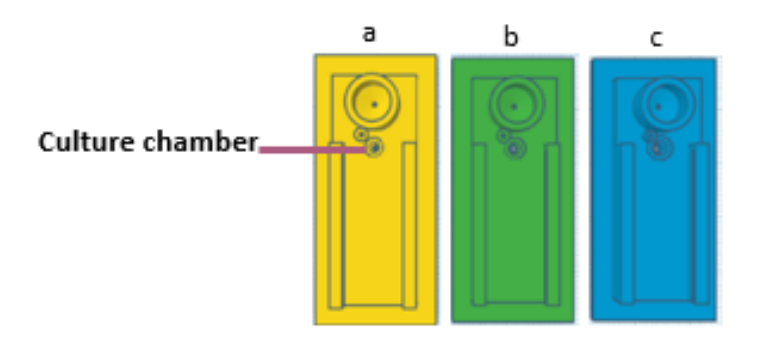


Figure 23. Version 5 model a to c.

This figure showed that culture chamber size increased from model a to c of version 5 of the 3D ForCell device.

The last version of device was made from black resin, as shown in figure 24. To be sure, we were able to stain and track spheroid with Cell Tracker clearly.



Figure 24. Black 3D ForCell device.

The black resin was used to print the 3D ForCell version 5.

Consequently, we have tried to take DIC and confocal images in the 3D ForCell device without oil and compare those images with images contained oil. In the last spheroid cultivation, we just seeded cells in ULA plates to grow spheroid. After spheroid formation, we transferred them to the 3D ForCell device in two conditions with and without oil. Both DIC and confocal images from the 3D ForCell without oil represented more clear and clean images from specimens (Figure 25. B) in comparison of 3D ForCell with oil (Figure 25. A). The confocal images were valid documents to prove spheroid structures existed in the 3D ForCell device and revealed affect the presence of oil in images clearly. Therefore, our modifications were useful and efficient to succeed in this project.

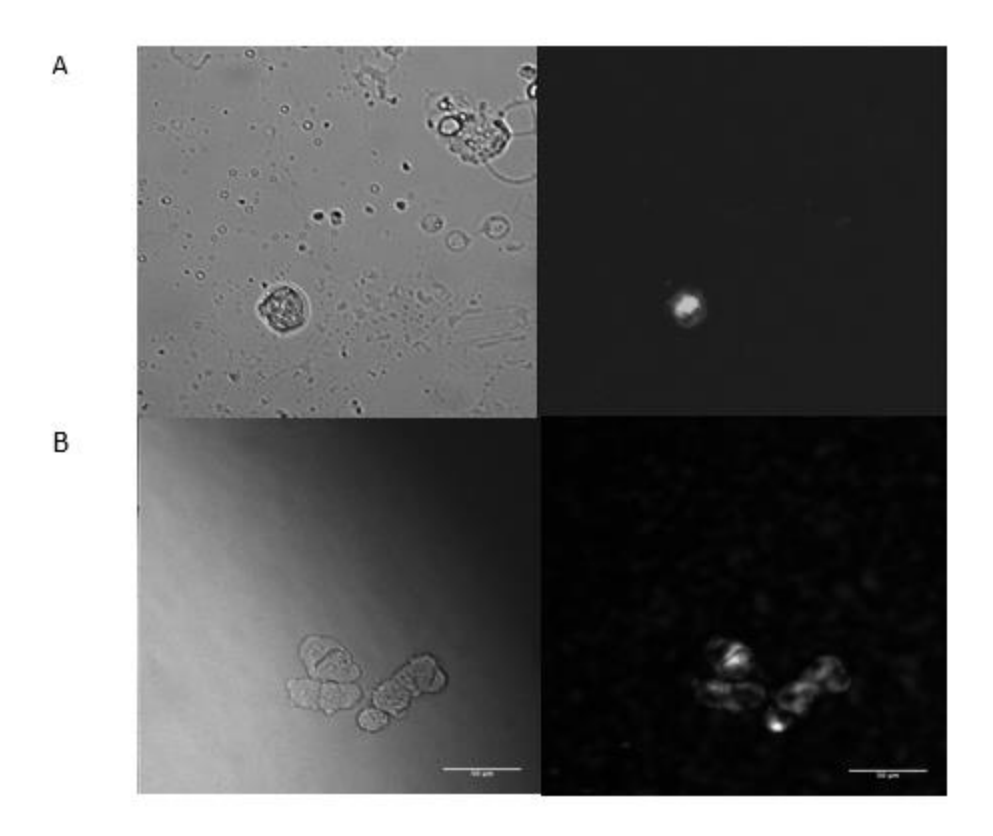


Figure 25. DIC and confocal images from spheroid into two different conditions.

A) The DIC and confocal images were taken from transferred spheroid into the 3D ForCell device in the usual condition.

B) The DIC and confocal images were taken from transferred spheroid into the 3D ForCell device, which oil/culture chamber just was filled with media.

4.4 Capillary pump

We used different filter papers with different thicknesses to assess the flow rate possible with different filter papers. We repeated this experiment in version 3, 5a, 5b, and 5c of our 3 models of version device and the results are present in figure 26. The first perfusion test in version 3 of the device a showed that filter paper grade 2 had the slowest flow rate in comparison to others and filter paper grade 3 had the faster flow rate to do media exchanging. This result was repeated in version 5a, 5b, and 5c. As for version 3 and all of the versions 5, filter paper grade 3 had the biggest perfusion rate followed by filter paper grade 5, 1, 2, respectively. The perfusion rate of filter paper grade 1 was slightly higher than filter paper grade 2, but not statistically significant in all versions.

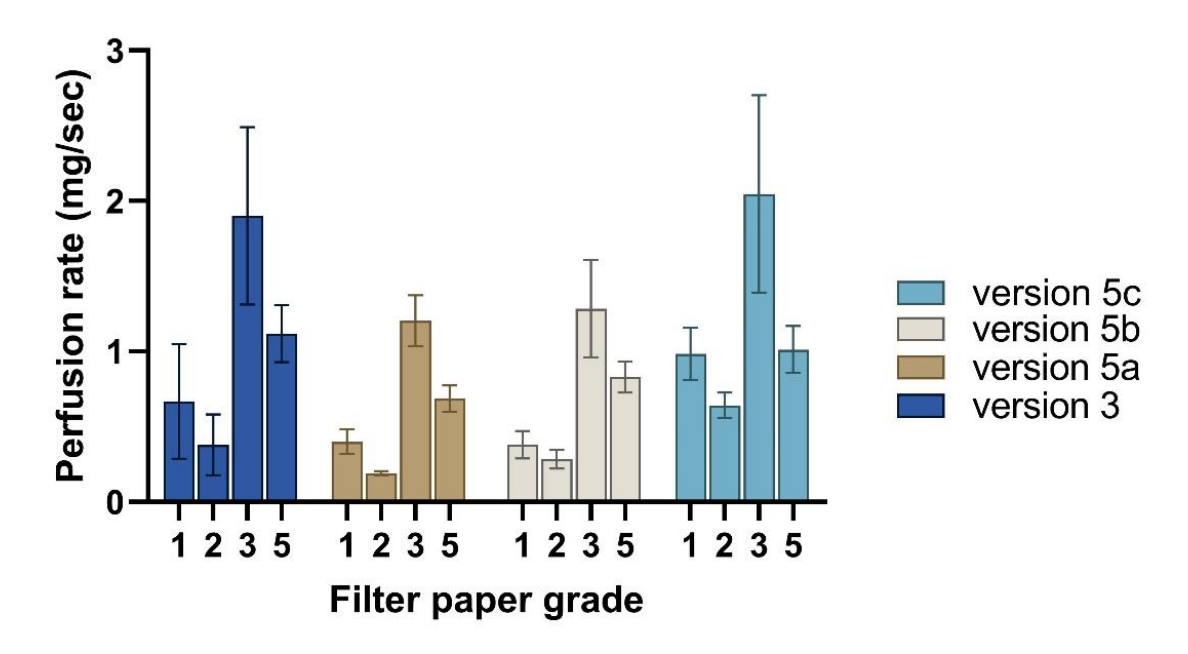


Figure 26. Perfusion rate of versions 3 and 5 of the 3D ForCell device.

2-way ANOVA showed that both filter paper grade and version/model of device have a statistically significant effect on the perfusion rate (p<0.0001). Our result also revealed that all versions of devices have a similar response to filter paper, but there is a difference between the amount of perfusion rate.

Section 5. Discussion

5 Discussion

5.1 Design

We had to make several modifications to the device's design so that it could be able to grow spheroids. Microscope observations are important to the study of biological samples. However, we found that the high thickness of the bottom oil chamber made microscopy observation difficult. After reducing the size of the oil chamber capacity from 170 μ l to 100 μ l, greatly facilitated microscopy observations. However, we found that the oil of the oil chamber still made acquisition of DIC and confocal microscopy images substantially more difficult.

The addition of a window made of optical plastic in the cover of the 3D ForCell devices made daily microscopy observations more comfortable. In addition, this updated cover design helped keep the devices sterile without the need to use a petri-dish to cover the device between the imaging sessions. Moreover, it could help us to improve imaging conditions and provided faster microscopy observation and taking images.

Both culture and media chamber's size was increased. The media chamber had 100 μ l volume capacity and it changed to 200 μ l in its final version. We supposed that the bigger media chamber could keep media for a longer time. Therefore, if the 3D ForCell device had a bit of media leakage through the microfluidic channel, adding more media was a good suggestion to minimize the negative impact of persevering cells every 2 days of media exchange.

To have more chances to get spheroid in the device, we have decided to seed higher cell density in the culture chamber. This was the primary driving force to increase the size of the culture chamber. Besides, we considered that the size of the culture chamber was too small to allow for the formation of the spheroid. Additionally, having a bigger culture chamber valve allowed us to seed cells from the top of the culture chamber (Figure 7. B).

The change in the air vent size was also a remarkable improvement. Indeed, the initial small size of the air vent led to oil/media leakage during the device's loading. The bigger air vent did not allow to do the perfusion test. So far, the medium size of air vent with 3 mm height and 1 mm diameter was the best choice without the mentioned problems.

In the final version of the device, we used glass coverslip instead of optical plastic coverslip in previous versions. It was clear that using glass coverslip was a moderate success to overcome the oil leakage issue. Moreover, glass coverslip compares to optical plastic coverslip was a good option to check cells under a microscope with higher resolution.

In the last version, a bigger frame with increasing size 10 mm in height and 5 mm in width was used in comparison to previous versions. That was because the smaller frame of device could not accommodate glass coverslip and that glass coverslip was broken easily after a small blow. The new frame could cover glass coverslip in the bottom of the device to prevent possible brake issues.

Finally, the black resin was used to print the last version of device. This black version was used to take confocal images that explained in section 4.3.4.

5.2 Printing and fabrication

There has been a leakage problem in several versions of the device, which we have tried to remove them using different solution ways during post-processing.

We tested different orientations to print new devices. Print devices from different angles helped us to evaluate which angle can minimize the number of overhangs, which is key to have a successful and precise print. We found that the best angle gives us less need to use sanding papers. We realized that the proper orientation to print is side-up with more angles. The angle reduced the possible damage during the cutting support section.

After 3D printing, the 3D ForCell devices were exposed under UV-source imager and UV-blue light with different exposure times. In this case, they evaluated how long it took to do resin polymerization, which should be considered a standard time for polymerization. The UV-blue light with 30 minutes could polymerize resin properly, which removed the polymerization problem in the 3D ForCell device.

Sanding papers with different grades were used to make a soft surface in the bottom of the device. The soft area helps to solve oil/media leakage between coverslip and device.

UV-glue was used to stick coverslip at the bottom of device. By using a UV-source imager, glue and devices have found more chances to cure. This step helps us to make sure there is no leakage issue in the next step.

Using UV-blue light and increasing exposure time could remove cracking problems on the top and the bottom of device. Sanding papers were used to remove oil/media leakage between a coverslip and the device. Using UV-glue and glass coverslip completely removed the oil leakage issue. All of these fabrication tricks helped us develop the 3D ForCell devices to obtain better results in the final version.

5.3 Growing spheroid

Before cell seeding, typically we used ethanol 70% to sterilize the 3D ForCell devices. Approximately after 2 days of cell seeding, some cracks appeared on the top and bottom of the devices. We assumed that ethanol 70% or heating of device in incubator could affect those devices. We modified the sterilization protocol to make sure ethanol is not the main factor for cracking issues. However, ethanol is generally using to clean resin after printing, so it could not be the issue. It is likely to consider the device fabrication method for making cracks. When all of the resin layers do not polymerize completely, they can make leakage issues in the 3D For Cell. This problem was solved by increasing UV exposure time, as we never had problems with devices cracking once we moved to more robust post-processing UV and blue-light exposure parameters.

Two types of cancer cell lines, A549 and MCF7, were used as cells for device cell seeding. Both of them are epithelial cells in which A549 derived from cancerous lung cells and MCF7 derived from breast cancer cells. These cancer cell lines were selected due to being well-established cell lines known to be able to produce spheroids in a variety of culture system[164], (Reviewed in [165]). Approximately 250.000 cells/ml of A549 cancer cells and 500.000 cells/ml of MCF7 were seeded on top of the culture chamber in the 3D ForCell device.

After several trials and errors, we finally succeeded in producing structures reassembling spheroid (Figure 21 in section 4.3.3.1). We were able to get spheroid in modified version 4 of the 3D ForCell. This DIC image (Figure 21 in section 4.3.3.1) showed spheroid structure that looked similar in the spheroids grown in ULA plates. Furthermore, it appeared with the same timeline for the spheroids grown in ULA plates. Although we were not able to stain spheroid into the device and were not sure that they were cells or debris. Because quality of the DIC was also deeply affected by the presence of oil.

Consequently, we compared taking microscopy images in both with and without oil conditions, from the spheroid in the black version of the device. We realized that both DIC and confocal images in device without oil condition was more clear and clean to track (Figure 25. B).

5.4 Capillary pump

Different Whatman filter papers with different thicknesses were used to media absorbance and finally did media exchanging. Because we did not want to disturb spheroid during media exchanging, we were looking to find filter paper with a slower flow rate. We found that filter paper grade 2 had slowest perfusion speed and was more proper to our aim.

We realized that model 5c had a slightly bigger flow rate, maybe due to having a bigger size of culture chamber in comparison to others, perhaps because of the bigger culture chamber providing bigger contact points.

Section 6. Conclusions and future perspectives

6 Conclusions and future perspectives

6.1 Conclusion

Our results demonstrated that the 3D ForCell device was able to keep and grow spheroids. This device has many advantages to use for spheroid cultivation. This device makes an opportunity to control input and output materials such as media, cells, and drugs. Besides, the 3D ForCell devices same as most of the microfluidic devices are less time and regent consuming. Therefore, these devices are more cost-effective and analytical efficient.

This device is home-made, which means it does not need to order and prepare it in industry. Every scientist who has a SLA 3D printer can manufacture the 3D ForCell in their own lab. Indeed, resin as the main material of this device is less expensive than other 3D print materials such as PDMS [166]. Therefore, the 3D ForCell fabrication is cheaper than other 3D printing devices. The way of print is easy and the scientist can be more independent without need to buy this device from the industry.

Before the 3D ForCell invention, some researchers introduced mesh barrier pipette tips for ULA plates to aspirate old media and add fresh media [167]. They assumed that by using this 3D-tip, ULA plates could be more appropriate to culture spheroid. However, several drawbacks come up in this method. For example, we have to transfer spheroid from ULA plates to small tubes for tracking cells and taking microscopy images. Although, this way can disturb spheroid shape. Additionally, changing the media by using 3D tips is not easy. 3D ForCell solved these problems because the growing, tracking, and imaging cell processes can happen in a single device.

Using a paper-based capillary pump is another option of the 3D ForCell device. This technology is user friendly and will not disturb the spheroid due to slower flow rate filter paper was selected to exchange media.

Adding fresh media is from the media chamber and through a microfluidic channel with a slow flow rate not from the top of well. Because this way of adding media from the top of well same as what is usual in ULA plates can disturb the spheroid shape.

ULA plates are disposable, but the 3D ForCell can reuse several times. It just should clean after using with cleaning protocol and sterilize again based on the approved sterilization method. However, we could not reuse most of them during trials and errors, but we could reuse several last version the 3D ForCell devices.

Moreover, the 3D ForCell device does not need an electrical pump to change media; it just needs appropriate filter paper to change media. This paper-based capillary pump is cheap and approval. This capillary pump was designed to test cancer drugs on culture spheroid in the 3D ForCell device. ULA plates do not have this option to use as an analysis cassette for drug testing.

That is right ULA plates have 96 wells with more chances to culture spheroid. However, if we can develop and finalize the 3D ForCell device correctly, we can make a platform with more wells. In this case, the 3D ForCell device will have more wells to grow spheroid.

We had a lot of challenges to develop the 3D ForCell and reach the point to get spheroid into the device. Now this device is ready to grow spheroid but needs more validation to obtain some results in several times.

6.2 Future perspectives

We began spheroid cultivation in the 3D ForCell device and we succeeded in creating spheroid in the 3D ForCell device (Figure 21 in section 4.3.3.1). As A549 spheroid structure has been observed in the 3D ForCell devices after 5 days and it could preserve until 7 days. The next set of experiments would need to assess the ability of the 3D ForCell devices to culture spheroids for more extended periods. Such experiments would involve spheroid growing, cell viability, and do microscopy process for spheroid formed up to 15 days. In this case, we may have to optimize the 3D ForCell device to obtain good potential to survive cells up to 15 days.

To make sure those cells of spheroid preserve the nature of the first cancer tissues and still have functionality, we want to measure the amount of their tissue-specific marker expression over the course of 15 days of culture. Those tissue specific markers are surfactant protein C (SP-C) and alkaline phosphatase (ALP) for A549 and MCF7, respectively. Because A549 cells secrete SP-C marker, we can measure this marker when secreted in the culture chamber with a paper-based capillary pump after 15 days of cell seeding. Due to ALP being not secreted by the cells, we could evaluate ALP expression by preparing spheroid slices by the use of a microtome followed by histochemistry tests such as H&E staining and immunohistochemistry (Section 3.7.3) we will able to evaluate ALP expression in MCF7 spheroids. We can evaluate spheroid cell functionality after 15 days of cell seeding in the 3D ForCell device. Additionally, we could compare spheroid cells differentiation in the 3D ForCell device with ULA plates.

We have performed preliminary confocal fluorescence microscopy on A549 spheroids (Figure 25 in section 4.3.4). Imaging in the devices or through large spheroid structures comes with its own set of challenges. One of the first set of additional experiments should be focused at optimizing confocal microscopy imaging in the 3D ForCell device in both live and fixed imaging settings.

In addition, we could visualize collagen [168] deposition with a confocal microscope. Electron microscopy opens many doors for scientists; it would be worthwhile to assess the ultrastructure organization of spheroid models with this microscope. We want to compare spheroid

ultrastructure, including collagen fibrils throughout the culture on spheroids in the 3D ForCell device and ULA plates.

Other types of oil instead of HT200 oil will replace with more or less densities to improve the quality of microscopy images. Other suggestions are using media instead of oil in the 3D ForCell devices and applying for low attachment surface coverslip instead of glass coverslip at the bottom of 3D ForCell device. We would like to take microscopy images from cultivated spheroid in the 3D ForCell device in all of the above conditions and evaluate the quality of spheroid in these new conditions.

We would plan to use different filter papers with different agarose concentrations (1,3,5%) as a common material to provide a slow absorbance flow rate. Agarose with desired concentration can be heated to melt and penetrate porous filter papers (Reviewed in [169]). Different concentrations of agarose can block different percentage of pores of filter paper. After testing filter paper, filter paper with a slower flow rate will select to change media.

As we could just try the 3D ForCell to grow two more common types of cancer cell lines, we will culture other types of cancerous cell lines such as bone or colorectal cells. Due to organoids can be used as human disease modeling in the lab environment, this would be a good idea to start culturing organoid from different tissues in the 3D ForCell device. For instance, intestine organoids can be created in the 3D ForCell due to its many cell structures and can be recapitulated part of the real intestinal tissue in the human body [170]. Therefore, the 3D ForCell will allow more chances to expand human organ modeling in the lab environment with more control on cell density, fluids, and media.

If successful, the experiments listed above will expand our knowledge to develop and validate 3D ForCell device as a valid tool in the 3D cell culture and tissue engineering.

References

- 1. Hynes, R.O., *The extracellular matrix: not just pretty fibrils.* Science, 2009. **326**(5957): p. 1216-9.
- 2. Vlahopoulos, S.A., et al., *Dynamic aberrant NF-kappaB spurs tumorigenesis:* a new model encompassing the microenvironment. Cytokine Growth Factor Rev, 2015. **26**(4): p. 389-403.
- 3. Gorfinkiel, N., et al., *Mechanical control of global cell behaviour during dorsal closure in Drosophila*. Development, 2009. **136**(11): p. 1889-98.
- 4. Cooper, G.M., The Cell: A Molecular Approach Hardcover. 2000.
- 5. Gilbert, S.F., Development biology. 2000.
- 6. Dorsky, R.I., et al., *Regulation of neuronal diversity in the Xenopus retina by Delta signalling*. Nature, 1997. **385**(6611): p. 67-70.
- 7. Alberts, B., Molecular Biology of the Cell. 2002.
- 8. Goodenough, D.A. and D.L. Paul, *Gap junctions*. Cold Spring Harb Perspect Biol, 2009. **1**(1): p. a002576.
- 9. Perrimon, N. and M. Bernfield, *Cellular functions of proteoglycans--an overview*. Semin Cell Dev Biol, 2001. **12**(2): p. 65-7.
- 10. rozario, t., the extracellular matrix in development and morphogenesis: a dynamic view. 2009.
- 11. Fratzi, P., *Collagen: structure and mechanics, an introduction.* Springer, 2008.
- 12. Pawelec, K.M., S.M. Best, and R.E. Cameron, *Collagen: a network for regenerative medicine*. Journal of Materials Chemistry B, 2016. **4**(40): p. 6484-6496.
- 13. Gelse, K., E. Poschl, and T. Aigner, *Collagens--structure, function, and biosynthesis*. Adv Drug Deliv Rev, 2003. **55**(12): p. 1531-46.
- 14. Mancera, N.S.G.R.L., *The Structure of Glycosaminoglycans and their Interactions with Proteins.* chemical biology& Drug design, 2008.
- 15. Lozzo, R.V., *Proteoglycan form and function:A comprehensive nomenclature of proteoglycans.* Science direct, 2015. **42**.
- 16. Proudfoot, A.E.I., et al., *Glycosaminoglycan Interactions with Chemokines Add Complexity to a Complex System.* Pharmaceuticals (Basel), 2017. **10**(3).
- 17. mescher, a.L., Junquiera's basic histology. 2015.
- 18. ricardo, *The role of fibronectin laminin vitronectin and their receptors on cellular adhesion in proliferative.* 1994.
- 19. Singh, P., C. Carraher, and J.E. Schwarzbauer, *Assembly of fibronectin extracellular matrix*. Annu Rev Cell Dev Biol, 2010. **26**: p. 397-419.

- 20. Linask, K.K. and J.W. Lash, *A role for fibronectin in the migration of avian precardiac cells. I. Dose-dependent effects of fibronectin antibody.* Dev Biol, 1988. **129**(2): p. 315-23.
- 21. Tsang, K.Y., et al., *The developmental roles of the extracellular matrix:* beyond structure to regulation. Cell Tissue Res, 2010. **339**(1): p. 93-110.
- 22. Hogg, N., Integrins. 1998.
- 23. Li, J. and T.A. Springer, *Integrin extension enables ultrasensitive regulation* by cytoskeletal force. Proc Natl Acad Sci U S A, 2017. **114**(18): p. 4685-4690.
- 24. Docheva, D., et al., *Human mesenchymal stem cells in contact with their environment: surface characteristics and the integrin system.* J Cell Mol Med, 2007. **11**(1): p. 21-38.
- 25. Mitra, S.K., D.A. Hanson, and D.D. Schlaepfer, *Focal adhesion kinase: in command and control of cell motility.* Nat Rev Mol Cell Biol, 2005. **6**(1): p. 56-68.
- 26. Lu, S. and Y. Wang, *Single-cell imaging of mechanotransduction in endothelial cells*. Prog Mol Biol Transl Sci, 2014. **126**: p. 25-51.
- 27. Qin, J., O. Vinogradova, and E.F. Plow, *Integrin bidirectional signaling: a molecular view.* PLoS Biol, 2004. **2**(6): p. e169.
- 28. Brown, N.H., et al., *Talin is essential for integrin function in Drosophila.* Dev Cell, 2002. **3**(4): p. 569-79.
- 29. Seetharaman, S. and S. Etienne-Manneville, *Integrin diversity brings* specificity in mechanotransduction. Biol Cell, 2018. **110**(3): p. 49-64.
- 30. Timpson, P., et al., Coordination of cell polarization and migration by the Rho family GTPases requires Src tyrosine kinase activity. Curr Biol, 2001. **11**(23): p. 1836-46.
- 31. Zamir, E. and B. Geiger, *Focal Adhesions and Related Integrin Contacts*. 2013. p. 318-323.
- 32. Harrison, R.G., *Observations of the living developing nerve fiber.* the Society for Experimental Biology and Medicine, 1907.
- 33. Breslin, S. and L. O'Driscoll, *Three-dimensional cell culture: the missing link in drug discovery.* Drug Discov Today, 2013. **18**(5-6): p. 240-9.
- 34. Invitrogen, G.c., *Cell culture basics*.
- 35. Kapalczynska, M., et al., 2D and 3D cell cultures a comparison of different types of cancer cell cultures. Arch Med Sci, 2018. **14**(4): p. 910-919.
- 36. Abbott, A., *Cell culture: biology's new dimension.* Nature, 2003. **424**(6951): p. 870-2.

- 37. DiMasi, J.A. and H.G. Grabowski, *Economics of New Oncology Drug Development*. 2007. **25**(2): p. 209-216.
- 38. Friedrich, J., R. Ebner, and L.A. Kunz-Schughart, *Experimental anti-tumor therapy in 3-D: spheroids--old hat or new challenge?* Int J Radiat Biol, 2007. **83**(11-12): p. 849-71.
- 39. Rozario, T. and D.W. DeSimone, *The extracellular matrix in development and morphogenesis: a dynamic view.* Dev Biol, 2010. **341**(1): p. 126-40.
- 40. Lee, G.Y., et al., *Three-dimensional culture models of normal and malignant breast epithelial cells.* Nat Methods, 2007. **4**(4): p. 359-65.
- 41. Pampaloni, F., E.G. Reynaud, and E.H. Stelzer, *The third dimension bridges the gap between cell culture and live tissue.* Nat Rev Mol Cell Biol, 2007. **8**(10): p. 839-45.
- 42. Langhans, S.A., *Three-Dimensional in Vitro Cell Culture Models in Drug Discovery and Drug Repositioning*. Front Pharmacol, 2018. **9**: p. 6.
- 43. Yari, A., et al., The role of biodegradable engineered random polycaprolactone nanofiber scaffolds seeded with nestin-positive hair follicle stem cells for tissue engineering. Adv Biomed Res, 2016. **5**: p. 22.
- 44. Ghasemi-Mobarakeh, L., et al., *Structural properties of scaffolds: Crucial parameters towards stem cells differentiation.* World J Stem Cells, 2015. **7**(4): p. 728-44.
- 45. Tibbitt, M.W. and K.S. Anseth, *Hydrogels as extracellular matrix mimics for 3D cell culture.* Biotechnol Bioeng, 2009. **103**(4): p. 655-63.
- 46. Nikolova, M.P. and M.S. Chavali, *Recent advances in biomaterials for 3D scaffolds: A review.* Bioact Mater, 2019. **4**: p. 271-292.
- 47. Phani, K.K., The relations between the shear modulus, the bulk modulus, and Young's modulus for porous isotropic ceramic materials. Materials science and engineering, 2008. **490**.
- 48. Fan, D., U. Staufer, and A. Accardo, *Engineered 3D Polymer and Hydrogel Microenvironments for Cell Culture Applications*. Bioengineering (Basel), 2019. **6**(4).
- 49. Sun, M., et al., Extracellular matrix stiffness controls osteogenic differentiation of mesenchymal stem cells mediated by integrin α5. Stem Cell Research & Therapy, 2018. **9**(1): p. 52.
- 50. Engler, A.J., et al., *Matrix elasticity directs stem cell lineage specification*. Cell, 2006. **126**(4): p. 677-89.
- 51. Lawrence, B.J. and S.V. Madihally, *Cell colonization in degradable 3D porous matrices*. Cell Adh Migr, 2008. **2**(1): p. 9-16.

- 52. Karageorgiou, V. and D. Kaplan, *Porosity of 3D biomaterial scaffolds and osteogenesis.* Biomaterials, 2005. **26**(27): p. 5474-91.
- 53. Amoabediny, G., The Role of Biodegradable Engineered Scaffold in Tissue Engineering. 2011.
- 54. Liu, X., J.M. Holzwarth, and P.X. Ma, Functionalized synthetic biodegradable polymer scaffolds for tissue engineering. Macromol Biosci, 2012. **12**(7): p. 911-9.
- 55. Zhu, J. and R.E. Marchant, *Design properties of hydrogel tissue-engineering scaffolds*. Expert Rev Med Devices, 2011. **8**(5): p. 607-26.
- 56. Persikov, A.V., et al., *Amino acid propensities for the collagen triple-helix.* Biochemistry, 2000. **39**(48): p. 14960-7.
- 57. Silver, F.H., *Collagen self-assembly and the development of tendon mechanical properties.* Biomechanics, 2003.
- 58. Dinescu, S., et al., *Collagen-Based Hydrogels and Their Applications for Tissue Engineering and Regenerative Medicine*. 2018. p. 1-21.
- 59. Wolf, K., et al., *Collagen-based cell migration models in vitro and in vivo.* Semin Cell Dev Biol, 2009. **20**(8): p. 931-41.
- 60. Reynolds, D.S., et al., *Breast Cancer Spheroids Reveal a Differential Cancer Stem Cell Response to Chemotherapeutic Treatment*. Sci Rep, 2017. **7**(1): p. 10382.
- 61. Dong, C. and Y. Lv, Application of Collagen Scaffold in Tissue Engineering: Recent Advances and New Perspectives. Polymers (Basel), 2016. **8**(2).
- 62. Vukicevic, S., et al., Identification of multiple active growth factors in basement membrane Matrigel suggests caution in interpretation of cellular activity related to extracellular matrix components. Exp Cell Res, 1992.

 202(1): p. 1-8.
- 63. Cao, F., et al., *In vivo imaging and evaluation of different biomatrices for improvement of stem cell survival.* J Tissue Eng Regen Med, 2007. **1**(6): p. 465-8.
- 64. Park, Y.S., et al., Differentiated tonsil-derived mesenchymal stem cells embedded in Matrigel restore parathyroid cell functions in rats with parathyroidectomy. Biomaterials, 2015. **65**: p. 140-52.
- 65. Lombardo, Y., et al., *Nicastrin regulates breast cancer stem cell properties and tumor growth in vitro and in vivo.* Proc Natl Acad Sci U S A, 2012. **109**(41): p. 16558-63.
- 66. Ootani, A., Sustained in vitro intestinal epithelial culture within a Wnt-dependent stem cell niche. Nature medicine, 2009. **15,701-706**.

- 67. Gill, B.J. and J.L. West, *Modeling the tumor extracellular matrix: Tissue engineering tools repurposed towards new frontiers in cancer biology.* J Biomech, 2014. **47**(9): p. 1969-78.
- 68. Lv, D., et al., *Three-dimensional cell culture: A powerful tool in tumor research and drug discovery.* Oncol Lett, 2017. **14**(6): p. 6999-7010.
- 69. Krug, C., et al., Fibrin glue displays promising in vitro characteristics as a potential carrier of adipose progenitor cells for tissue regeneration. J Tissue Eng Regen Med, 2019. **13**(3): p. 359-368.
- 70. Kouhbananinejad, S.M., et al., A fibrinous and allogeneic fibroblast-enriched membrane as a biocompatible material can improve diabetic wound healing. Biomater Sci, 2019. **7**(5): p. 1949-1961.
- 71. Elliott, M.B., Regenerative and durable small-diameter graft as an arterial conduit. PANS, 2019.
- 72. Goldfracht, I., et al., Engineered heart tissue models from hiPSC-derived cardiomyocytes and cardiac ECM for disease modeling and drug testing applications. Acta Biomater, 2019. **92**: p. 145-159.
- 73. Mallik, A., *Biodegradability and biocompatibility of natural polymers*. Vol. 133-168. 2019.
- 74. Deller, R.C., et al., *Artificial cell membrane binding thrombin constructs* drive in situ fibrin hydrogel formation. Nat Commun, 2019. **10**(1): p. 1887.
- 75. Ahmed, T.A., E.V. Dare, and M. Hincke, *Fibrin: a versatile scaffold for tissue engineering applications*. Tissue Eng Part B Rev, 2008. **14**(2): p. 199-215.
- 76. Kim, O.V., et al., *Foam-like compression behavior of fibrin networks*. Biomech Model Mechanobiol, 2016. **15**(1): p. 213-228.
- 77. Wang, X., et al., *Gelatin-Based Hydrogels for Organ 3D Bioprinting*. Polymers (Basel), 2017. **9**(9).
- 78. Afewerki, S., et al., *Gelatin-polysaccharide composite scaffolds for 3D cell culture and tissue engineering: Towards natural therapeutics.* Bioeng Transl Med, 2019. **4**(1): p. 96-115.
- 79. Jung, J.W., et al., A new method of fabricating a blend scaffold using an indirect three-dimensional printing technique. Biofabrication, 2015. **7**(4): p. 045003.
- 80. Fu, Y., et al., 3D cell entrapment in crosslinked thiolated gelatin-poly(ethylene glycol) diacrylate hydrogels. Biomaterials, 2012. **33**(1): p. 48-58.

- 81. Song, K., et al., Fabrication and Cell Responsive Behavior of Macroporous PLLA/Gelatin Composite Scaffold with Hierarchical Micro-Nano Pore Structure. Nanomaterials (Basel), 2015. **5**(2): p. 415-424.
- 82. Asti, A. and L. Gioglio, *Natural and synthetic biodegradable polymers:*different scaffolds for cell expansion and tissue formation. Int J Artif Organs, 2014. **37**(3): p. 187-205.
- 83. Zhang, Y.S. and A. Khademhosseini, *Advances in engineering hydrogels*. Science, 2017. **356**(6337).
- 84. A.Langhans, S., *3D in vitro cell culture models in drug discovery and drug repositioning.* Frontiers in pharmacology, 2018. **10.3389**.
- 85. Mohamed, F. and C.F. van der Walle, Engineering biodegradable polyester particles with specific drug targeting and drug release properties. J Pharm Sci, 2008. **97**(1): p. 71-87.
- 86. Emami, F., S.J. Mostafavi Yazdi, and D.H. Na, *Poly(lactic acid)/poly(lactic-co-glycolic acid) particulate carriers for pulmonary drug delivery*. Journal of Pharmaceutical Investigation, 2019. **49**(4): p. 427-442.
- 87. Kundu, J., F. Pati, and Y.H. Jeong, *Biomaterials for Biofabrication of 3D Tissue Scaffolds*. 2013. p. 23-46.
- 88. Bergsma, E.J., et al., Foreign body reactions to resorbable poly(L-lactide) bone plates and screws used for the fixation of unstable zygomatic fractures. J Oral Maxillofac Surg, 1993. **51**(6): p. 666-70.
- 89. Ignatius, A.A. and L.E. Claes, *In vitro biocompatibility of bioresorbable polymers: poly(L, DL-lactide) and poly(L-lactide-co-glycolide).* Biomaterials, 1996. **17**(8): p. 831-9.
- 90. Nath, S. and G.R. Devi, *Three-dimensional culture systems in cancer research: Focus on tumor spheroid model.* Pharmacol Ther, 2016. **163**: p. 94-108.
- 91. Alghuwainem, A., Scaffold free 3D cell sheet technique bridges the gap between 2D cell culture and animal model. Molecular science, 2019.
- 92. Simian, M. and M.J. Bissell, *Organoids: A historical perspective of thinking in three dimensions.* J Cell Biol, 2017. **216**(1): p. 31-40.
- 93. Takebe, T., et al., *Vascularized and functional human liver from an iPSC-derived organ bud transplant*. Nature, 2013. **499**(7459): p. 481-484.
- 94. Gonzalez, L.M., et al., *Cell lineage identification and stem cell culture in a porcine model for the study of intestinal epithelial regeneration.* PLoS One, 2013. **8**(6): p. e66465.

- 95. Elkabetz, Y., et al., *Human ES cell-derived neural rosettes reveal a functionally distinct early neural stem cell stage.* Genes Dev, 2008. **22**(2): p. 152-65.
- 96. Fatehullah, A., S.H. Tan, and N. Barker, *Organoids as an in vitro model of human development and disease.* Nat Cell Biol, 2016. **18**(3): p. 246-54.
- 97. Sachs, N., et al., *A Living Biobank of Breast Cancer Organoids Captures Disease Heterogeneity*. Cell, 2018. **172**(1-2): p. 373-386 e10.
- 98. Xu, H., et al., *Organoid technology and applications in cancer research*. Journal of Hematology & Oncology, 2018. **11**(1): p. 116.
- 99. Mullenders, J., et al., *Mouse and human urothelial cancer organoids: A tool for bladder cancer research.* Proc Natl Acad Sci U S A, 2019. **116**(10): p. 4567-4574.
- 100. Xu, X., M.C. Farach-Carson, and X. Jia, *Three-dimensional in vitro tumor models for cancer research and drug evaluation*. Biotechnol Adv, 2014. **32**(7): p. 1256-1268.
- 101. Zanoni, M., et al., 3D tumor spheroid models for in vitro therapeutic screening: a systematic approach to enhance the biological relevance of data obtained. Scientific Reports, 2016. **6**(1): p. 19103.
- 102. Elje, E., et al., *The comet assay applied to HepG2 liver spheroids.* Mutat Res, 2019. **845**: p. 403033.
- 103. Leite, P.E.C., et al., Suitability of 3D human brain spheroid models to distinguish toxic effects of gold and poly-lactic acid nanoparticles to assess biocompatibility for brain drug delivery. Particle and Fibre Toxicology, 2019. **16**(1): p. 22.
- 104. Froehlich, K., et al., Generation of Multicellular Breast Cancer Tumor Spheroids: Comparison of Different Protocols. J Mammary Gland Biol Neoplasia, 2016. **21**(3-4): p. 89-98.
- 105. Alfoldi, R., Single Cell Mass Cytometry of Non-Small Cell Lung Cancer Cells Reveals Complexity of In Vivo and Three-Dimensional Models over the Petri-Dish. Cells, 2019. **1093**.
- 106. Chan, H.F., et al., Rapid formation of multicellular spheroids in doubleemulsion droplets with controllable microenvironment. Scientific Reports, 2013. **3**(1): p. 3462.
- 107. Lin, R.Z., et al., Dynamic analysis of hepatoma spheroid formation: roles of *E-cadherin and beta1-integrin*. Cell Tissue Res, 2006. **324**(3): p. 411-22.
- 108. Legate, K.R., S.A. Wickstrom, and R. Fassler, *Genetic and cell biological analysis of integrin outside-in signaling.* Genes Dev, 2009. **23**(4): p. 397-418.

- 109. Klapholz, B. and N.H. Brown, *Talin the master of integrin adhesions.* J Cell Sci, 2017. **130**(15): p. 2435-2446.
- 110. Cram, E.J., S.G. Clark, and J.E. Schwarzbauer, *Talin loss-of-function uncovers roles in cell contractility and migration in C. elegans.* J Cell Sci, 2003. **116**(Pt 19): p. 3871-8.
- 111. Costa, E., 3D tumor spheroids: an overview on the tools and techniques used for their analysis. Science direct, 2016. **34**.
- 112. Gong, X., et al., *Generation of Multicellular Tumor Spheroids with Microwell-Based Agarose Scaffolds for Drug Testing*. PLoS One, 2015. **10**(6): p. e0130348.
- 113. Berndtsson, M., et al., Acute apoptosis by cisplatin requires induction of reactive oxygen species but is not associated with damage to nuclear DNA. Int J Cancer, 2007. **120**(1): p. 175-80.
- 114. Reynolds, D.S., et al., *Breast Cancer Spheroids Reveal a Differential Cancer Stem Cell Response to Chemotherapeutic Treatment*. Scientific Reports, 2017. **7**(1): p. 10382.
- 115. Wang, T., et al., Leveraging and manufacturing in vitro multicellular spheroid-based tumor cell model as a preclinical tool for translating dysregulated tumor metabolism into clinical targets and biomarkers. Bioresources and Bioprocessing, 2020. **7**(1): p. 35.
- 116. Baptista, L.S., et al., Adult Stem Cells Spheroids to Optimize Cell Colonization in Scaffolds for Cartilage and Bone Tissue Engineering. Int J Mol Sci, 2018. **19**(5).
- 117. Fennema, E., et al., *Spheroid culture as a tool for creating 3D complex tissues*. Trends Biotechnol, 2013. **31**(2): p. 108-15.
- 118. C.Costa, E., *3D tumor spheroids: an overview on the tools and techniques used for their analysis.* Science direct, 2016. **34**.
- 119. Larson, B., 3D Cell Culture: A Review of Current Techniques. Biotek, 2015.
- 120. Kelm, J.M., et al., *Method for generation of homogeneous multicellular tumor spheroids applicable to a wide variety of cell types*. Biotechnol Bioeng, 2003. **83**(2): p. 173-80.
- 121. Bartosh, T.J. and J.H. Ylostalo, *Preparation of anti-inflammatory mesenchymal stem/precursor cells (MSCs) through sphere formation using hanging-drop culture technique*. Curr Protoc Stem Cell Biol, 2014. **28**: p. Unit 2B 6.

- 122. Stadler, M., et al., *Increased complexity in carcinomas: Analyzing and modeling the interaction of human cancer cells with their microenvironment.* Semin Cancer Biol, 2015. **35**: p. 107-24.
- 123. Bartosh, T., Aggregation of human mesenchymal stromal cells (MSCs) into 3D spheroids enhances their antiinflammatory properties. PANS, 2010. **107-31**.
- 124. de Ridder, L., M. Cornelissen, and D. de Ridder, *Autologous spheroid* culture: a screening tool for human brain tumour invasion. Crit Rev Oncol Hematol, 2000. **36**(2-3): p. 107-22.
- 125. Ashraf, M.N., et al., Advanced In Vitro HepaRG Culture Systems for Xenobiotic Metabolism and Toxicity Characterization. European Journal of Drug Metabolism and Pharmacokinetics, 2019. **44**(4): p. 437-458.
- 126. Dhandayuthapani, B., *Polymeric Scaffolds in Tissue Engineering Application*. Polymer science, 2011. **1687-9422**.
- 127. Ivascu, A. and M. Kubbies, *Rapid generation of single-tumor spheroids for high-throughput cell function and toxicity analysis.* J Biomol Screen, 2006. **11**(8): p. 922-32.
- 128. Imamura, Y., et al., *Comparison of 2D- and 3D-culture models as drugtesting platforms in breast cancer.* Oncol Rep, 2015. **33**(4): p. 1837-43.
- 129. Ryu, N.E., S.H. Lee, and H. Park, *Spheroid Culture System Methods and Applications for Mesenchymal Stem Cells.* Cells, 2019. **8**(12).
- 130. Souza, G.R., et al., *Three-dimensional tissue culture based on magnetic cell levitation*. Nat Nanotechnol, 2010. **5**(4): p. 291-6.
- 131. Jensen, C. and Y. Teng, *Is It Time to Start Transitioning From 2D to 3D Cell Culture?* Front Mol Biosci, 2020. **7**: p. 33.
- 132. Timm, D.M., et al., A high-throughput three-dimensional cell migration assay for toxicity screening with mobile device-based macroscopic image analysis. Scientific Reports, 2013. **3**(1): p. 3000.
- 133. Hong, J.W. and S.R. Quake, *Integrated nanoliter systems*. Nature Biotechnology, 2003. **21**(10): p. 1179-1183.
- 134. Grayson, A.C.R., *A review: MEMs technology for physiologically integrated devices.* Proceesings of IEEE, 2004. **92**.
- 135. Bhatia, S.N. and D.E. Ingber, *Microfluidic organs-on-chips*. Nature Biotechnology, 2014. **32**(8): p. 760-772.
- 136. Whitesides, G.M., *The origins and the future of microfluidics*. Nature, 2006. **442**(7101): p. 368-373.

- 137. Bennett, M.R., et al., *Metabolic gene regulation in a dynamically changing environment*. Nature, 2008. **454**(7208): p. 1119-1122.
- 138. Chen, Y.A., et al., Generation of oxygen gradients in microfluidic devices for cell culture using spatially confined chemical reactions. Lab Chip, 2011. **11**(21): p. 3626-33.
- 139. Chiu, D.T., et al., *Patterned deposition of cells and proteins onto surfaces by using three-dimensional microfluidic systems*. Proc Natl Acad Sci U S A, 2000. **97**(6): p. 2408-13.
- 140. Son, S., et al., *Direct observation of mammalian cell growth and size regulation*. Nat Methods, 2012. **9**(9): p. 910-2.
- 141. Cookson, S., et al., *Monitoring dynamics of single-cell gene expression over multiple cell cycles.* Mol Syst Biol, 2005. **1**: p. 2005 0024.
- 142. Yamanaka, Y.J., et al., *Cellular barcodes for efficiently profiling single-cell secretory responses by microengraving.* Anal Chem, 2012. **84**(24): p. 10531-6.
- 143. Tay, S., et al., Single-cell NF-κB dynamics reveal digital activation and analogue information processing. Nature, 2010. **466**(7303): p. 267-271.
- 144. SaurabhVyawahare, Miniaturization and Parallelization of Biological and Chemical Assays in Microfluidic Devices. Chemistry&biology, 2010. 17.
- 145. Harrison, M., Planner chips technology for miniaturization and integration of separation techniques into monitoring systems capillary on a chip. Chromatography, 1992. **593**.
- 146. Sorger, P.K., *Microfluidics closes in on point-of-care assays.* Nat Biotechnol, 2008. **26**(12): p. 1345-6.
- 147. Azizipour, N., Evolution of biochip technology: a review from lab-on-a-chip to organ-on-a-chip. MDPI, 2020. **11**.
- 148. Breslin, S. and L. O'Driscoll, *The relevance of using 3D cell cultures, in addition to 2D monolayer cultures, when evaluating breast cancer drug sensitivity and resistance.* Oncotarget, 2016. **7**(29): p. 45745-45756.
- 149. Dai, X., et al., 3D bioprinted glioma stem cells for brain tumor model and applications of drug susceptibility. Biofabrication, 2016. **8**(4): p. 045005.
- 150. Lv, D., et al., A three-dimensional collagen scaffold cell culture system for screening anti-glioma therapeutics. Oncotarget, 2016. **7**(35): p. 56904-56914.
- 151. Li, C., et al., *Cell type and culture condition-dependent alternative splicing in human breast cancer cells revealed by splicing-sensitive microarrays.* Cancer Res, 2006. **66**(4): p. 1990-9.

- 152. Ravi, M., et al., *3D cell culture systems: advantages and applications.* J Cell Physiol, 2015. **230**(1): p. 16-26.
- 153. Bulysheva, A.A., et al., Enhanced chemoresistance of squamous carcinoma cells grown in 3D cryogenic electrospun scaffolds. Biomed Mater, 2013. **8**(5): p. 055009.
- 154. Izzo, L., et al., Influence of the static magnetic field on cell response in a miniaturized optically accessible bioreactor for 3D cell culture. Biomedical Microdevices, 2019. **21**(1): p. 29.
- 155. Amann, A., et al., Development of an innovative 3D cell culture system to study tumour--stroma interactions in non-small cell lung cancer cells. PLoS One, 2014. **9**(3): p. e92511.
- 156. website, P. https://www.pinterest.ca/pin/819936675895355964/.
- 157. Farnie, G., et al., Novel cell culture technique for primary ductal carcinoma in situ: role of Notch and epidermal growth factor receptor signaling pathways. J Natl Cancer Inst, 2007. **99**(8): p. 616-27.
- 158. Harrison, H., et al., Regulation of breast cancer stem cell activity by signaling through the Notch4 receptor. Cancer Res, 2010. **70**(2): p. 709-18.
- 159. Rota, L.M., et al., *Determining mammosphere-forming potential:* application of the limiting dilution analysis. J Mammary Gland Biol Neoplasia, 2012. **17**(2): p. 119-23.
- 160. Shaw, F.L., et al., A detailed mammosphere assay protocol for the quantification of breast stem cell activity. J Mammary Gland Biol Neoplasia, 2012. **17**(2): p. 111-7.
- 161. Lupp, A., *Morphology and cytochrome P450 isoforms expression in precision-cut rat liver slices.* Science direct, 2001. **161**.
- 162. Yan, Z., et al., A Novel Organ Culture Model of Mouse Intervertebral Disc Tissues. Cells Tissues Organs, 2016. **201**(1): p. 38-50.
- 163. structure, D.p.s. https://all3dp.com/1/3d-printing-support-structures/.
- 164. Swain, R.J., et al., Assessment of cell line models of primary human cells by Raman spectral phenotyping. Biophys J, 2010. **98**(8): p. 1703-11.
- 165. Comsa, S., A.M. Cimpean, and M. Raica, *The Story of MCF-7 Breast Cancer Cell Line: 40 years of Experience in Research.* Anticancer Res, 2015. **35**(6): p. 3147-54.
- 166. Gong, H., et al., *Optical Approach to Resin Formulation for 3D Printed Microfluidics*. RSC Adv, 2015. **5**(129): p. 106621-106632.

- 167. Chen, M., M.-L. Vial, and J.A. St John, *3D-tips: user-friendly mesh barrier pipette tips for 3D-spheroid culture.* Journal of Biological Engineering, 2019. **13**(1): p. 80.
- 168. Xu, S., et al., *The role of collagen in cancer: from bench to bedside.* J Transl Med, 2019. **17**(1): p. 309.
- 169. Soum, V., *Programmable paper based microfluidic device for biomarker detections.* micromachines, 2019. **10**.
- 170. Serra, D., et al., *Self-organization and symmetry breaking in intestinal organoid development*. Nature, 2019. **569**(7754): p. 66-72.